



Development of a High Energy Density Micro-Lithium Ion Battery

A Major Qualifying Project

Submitted to the faculty

of

WORCESTER POLYTECHNIC INSTITUTE

In partial fulfillment of the requirements of the

Degree of Bachelor of Science

of Mechanical Engineering

and

Degree of Bachelor of Science

of Chemical Engineering

by:

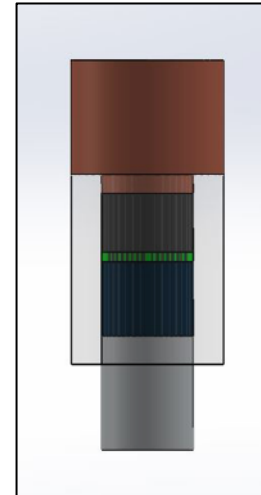
Chad Hucey (ME)

Omri Flaisher (ME)

Nathan Martel (ChE)

Approved:

Prof. Yan Wang, Project Advisor



Abstract

Micro-fabrication techniques have enabled production of increasingly compact electrical microsystems for applications ranging from distributed sensing and communication networks, to implantable medical devices. Micro-lithium ion battery technology lacks in size, performance, and manufacturability to power microelectronics that require equivalently sized energy sources. This project addresses a novel method for producing a low cost, micro-lithium ion battery, that utilizes 3D electrode structures, a polymer gel electrolyte separator, and a glass to metal sealed packaging design. The novel method employed in developing this micro-lithium ion battery yielded valuable information in progressing micro-battery technology, striving to develop a high energy density, micro-scale power source.

Acknowledgement

Completing this project would not have been possible without the assistance of several individuals who have provided us with necessary insight, expertise and assistance. We would like to extend our gratitude to the following individuals for their continued hard work and support:

To Professor Yan Wang, our project advisor, who has provided us with countless hours of expertise and feedback. Whenever we had an issue or concern, he always gave us numerous suggestions to try and solve the problem. He also gave us feedback on various aspects of the project so that we can improve our processing techniques, as well as avoid future problems.

To Zhangfeng Zheng and Qina Sa, two graduate students, who both have provided extensive expertise and feedback. When we had issues with our battery prototypes, they gave us potential reasons for the failures and methods to avoid these problems in the future. They both dedicated many hours to assisting us with our lab work and our electrochemical testing.

To Kevin Arruda, a graduate student who works in the Washburn machine shop, who assisted us with machining the components for our current collectors. He also gave us suggestions and feedback on methods of sealing our batteries.

To Roger Steele, the technical operations manager of the physics department, who loaned us our assembly rigs. He went out of his way to provide us with multiple pieces of equipment so that we could process several batteries simultaneously.

All of these individuals have given us invaluable assistance with our project and we owe the success of this project to their input and support.

Table of Contents

Abstract	2
Acknowledgement	3
Table of Contents	4
List of Figures	7
List of Tables	8
Executive Summary	9
1.0 Introduction	13
2.0 Background	15
2.1 Overview	15
2.2 History of Battery Technology Development	17
2.2.1 Early Batteries	17
2.2.2 Rechargeable Batteries	19
2.3 Battery Packaging	20
2.3.1 Cylindrical Cell	21
2.3.2 Button Cells	22
2.3.3 Prismatic Cells	23
2.3.4 Pouch Cell	24
2.4 Current Collectors	25
2.5 Electrodes	27
2.5.1 Anodes	28
2.5.2 Cathodes	30
2.5.3 Three-Dimensional Electrodes	32
2.6 Electrolytes and Separators	33
2.6.1 Electrolytes	33
2.6.2 Separators	34
2.7 Safety Concerns	36
2.7.1 Failure Mitigation	37
2.8 Current State of Micro-Battery Technology	38
2.8.1 Commercial Micro-Batteries	38
2.8.2 First 3-D Rechargeable Li Ion Micro-battery	39

2.8.3 3D Inter-digitated Li-Ion Micro-Battery Architectures (Sun).....	41
2.8.4 High Energy Density Micro-Battery Enabled by 3D Electrode and Micro-Packaging (Lai).....	42
2.8.5 Our Micro-Battery: Low Cost, 3D Electrode Micro-battery.....	43
3.0 Methodology.....	45
3.1 Development and Processing of Battery Packaging and External Components.....	45
3.1.1 Battery Housing.....	45
3.1.2 Selection / Preparation of Current Collectors.....	46
3.1.3 Aluminum Current Collector.....	46
3.1.4 Copper Current Collector.....	47
3.1.5 Machining Copper Rod.....	48
3.1.6 Adhesive Sealant.....	48
3.1.7 Hermeticity Testing of Battery Packaging.....	48
3.2 Development and Processing of Internal Battery Components.....	49
3.2.1 Polymer Gel Electrolyte Separator.....	49
3.2.1 Anode.....	50
3.2.2 Cathode.....	51
3.2.4 Measuring the Mass per Droplet of the Active Materials.....	52
3.3 Assembly and Packaging of Battery Unit.....	53
3.3.1 Initial Half Assembled Cell.....	53
3.3.2 Assembling the Half Cell.....	53
3.3.3 Assembly of Internal Battery Materials.....	54
3.3.4 Final Processing.....	58
3.3.5 Final Sealing.....	58
3.3.6 Light Shielding.....	58
3.4 Battery Testing.....	59
4.0 Results & Discussion.....	62
4.1 Determining the Allowable Internal Stress of the Glass Battery Housing.....	62
4.1.1 Calculating the Hoop Stress, σ_t	63
4.1.2 Calculating the Radial Stress, σ_r	64
4.1.3 Calculating the Longitudinal Stress, σ_l	65

4.2 Hermiticity and Component Testing	66
4.2.1 Hermiticity	66
4.2.2 Electrode Droplet Mass Testing	67
4.2.3 Current Collector Resistance	67
4.3 Polymer Gel Electrolyte Testing Results	68
4.4 Battery Capacity Testing	71
4.4.1 Theoretical Calculations	71
4.4.2 First Battery Using Stacking Method	72
4.4.3 Dripped Anode No Separator Method	74
4.4.4 Dripped Anode Using PGE	77
4.5 Challenges Associated With Micro-Battery	79
4.5.1 Sealing the Battery	79
4.5.2 Processing the Cell	81
5.0 Conclusions & Recommendations	83
5.1 Conclusions from Battery Testing	83
5.2 Recommendations for Future Work	84
5.2.1 Optimizing Current Packaging Design	85
5.2.2 Optimizing Current Processing Design	85
5.2.3 Mold Materials and Manufacturing Techniques	86
References	88
Appendices	92
Appendix A: Summary of Historical discoveries	92
Appendix B: Targray's Portfolio of Graphite Active Materials	93
Appendix C: A Comparison of Various Cathodes	94
Appendix D: Safety Hazards of Batteries	96
Appendix E: Aluminum Current Collector Information	100
Appendix F: Copper Current Collector Specifications	102
Appendix G: Epoxy Specifications	105
Appendix H: Pyrex Glass Technical information	110
Appendix I: Solution Stacking Method of Battery Assembly	113

List of Figures

Figure 1: Diagram of a battery circuit.....	16
Figure 2: Energy densities of various batteries types	17
Figure 3: A Parthian battery.....	18
Figure 4: Configuration of Volta's battery	18
Figure 5: Cross section of a Li-ion cylindrical cell.....	21
Figure 6: Popular 18650 li-ion cell	22
Figure 7: Button cells.....	23
Figure 8: Prismatic cell	24
Figure 9: Pouch cell	24
Figure 10: Simple battery configuration which highlights the placement of the current collectors	26
Figure 11: The three layer sandwiched PGE developed by H.P. Zhang et al (Zhang, 2007).....	35
Figure 12: Panasonic pin battery.....	38
Figure 13: Panasonic NBL micro-battery	39
Figure 14: Panasonic CR1025 coin battery	39
Figure 15: Substrate schematic	40
Figure 16: Improvements of 3D electrode micro-battery capacity	40
Figure 17: Optical and SEM images of the printed 16-layer interdigitated battery.....	42
Figure 18: Fully packaged assembly.....	42
Figure 19: Thin film micro-battery	43
Figure 20: SolidWorks model of our proposed micro-battery.....	44
Figure 21: Aluminum current collector being sanded	46
Figure 22: Aluminum dowel pin current collector after sanding to insure interference fit (Left) Copper current collector after machining and sanding (Right)	47
Figure 23: Lithium metal sealed inside battery prior to hermiticity test.....	49
Figure 24: Homogeneous PMMA/PVDF PGE film prior to electrolyte saturation.....	50
Figure 25: Electrode components from left to right: Conductive Graphite, LiCoO ₂ Powder, C65 Carbon, 2.5% Binder Solution of PVDF in NMP.....	51
Figure 26: 6 Drops of electrode were deposited on a glass slide and then allowed to dry. The total mass of electrode material was measured, then divided by 6 to estimate the mass of each droplet of electrode.....	52
Figure 27: Aluminum dowel pin current collector prior to sealing. Dowel pin and glass cylinder form a interference fit.	53
Figure 28: Alligator clip assembly rig for micro-batteries	54
Figure 29: Final product of cathode injection into the battery housing. Actual process (Left) Schematic of the process (Right)	55
Figure 30: LED backlit image of gap separator battery.....	56
Figure 31: PGE injected into battery to dry on top of cathode and form to battery casing. After drying, PGE will be saturated with liquid electrolyte to form gel. Actual process (Left) Schematic of process (Right).....	57
Figure 32: Post processing images of anode deposition onto copper current collect. Actual process (Left) Schematic of process (Right).....	57
Figure 33: Top Left: Fully assembled PGE separator battery. Top Right: Fully assembled gap separator battery. Bottom: Micro-battery with electrical tape wrapping for light shielding	59

Figure 34: The ARBIN electrochemical testing system with testing module and computer shown	60
Figure 35: Screen shot of the charging test design screen from the ARBIN software	61
Figure 36: Schematic of internal stress analysis	63
Figure 37: Graph of hoop stress vs internal pressure	64
Figure 38: Graph of radial stress vs internal stress	65
Figure 39: Longitudinal Stress	65
Figure 40: Graph of longitudinal stress vs internal stress	65
Figure 41: The sample of lithium metal is still present after 2 weeks of being submerged in 3 inches of water	66
Figure 42: Resistance testing of current collector materials	67
Figure 43: Charging curve test results for PGE separator in Swagelok cell at C/10 charge rate ..	69
Figure 44: Charging curve test results for PGE separator in Swagelok cell at C/5 charge rate ...	69
Figure 45: Charging curve test results for PGE separator in Swagelok cell at C/1 charge rate ...	70
Figure 46: Charging capacity test results for PGE separator in Swagelok cell at C/1 charging rate, capacity is greatly diminished after 30 cycles	70
Figure 47: Charging curve test results for an extensively short-circuited battery	73
Figure 48: Charging curve test results for a slightly short-circuited battery with other failure mechanisms possible	74
Figure 49: Voltage and Current vs Time for the gap separator battery	75
Figure 50: Charge capacity (Blue) for the gap separator battery	76
Figure 51: Discharge capacity (Blue) for the gap separator battery	77
Figure 52: Results of battery test for dripped anode battery assembly method utilizing a PGE separator	78
Figure 53: Example of a battery housing breaking during processing	81
Figure 54: Cost of Individual cathode components	95
Figure 55: Externally short-circuited cell	99
Figure 56: Aluminum dowel pin	100
Figure 57: Drawing of the dowel pin	100
Figure 58: Unprocessed Copper Rod	102
Figure 59: Drawing of the copper rod	103
Figure 60: Loctite epoxy	105

List of Tables

Table 1: Comparison of various current collector materials	26
Table 2: Remarks on various anode materials	30
Table 3: Summary of Droplet Mass Approximation Test	67
Table 4: Summary of Historical Findings	92
Table 5: Targray's Portfolio of Graphite Active Materials	93
Table 6: A Comparison of Various Cathode Materials	94
Table 7: Chart of Aluminum Properties	101
Table 8: Chart of Copper Alloy Properties	103
Table 9: Features and Benefits of Epoxy	105

Executive Summary

Microelectronics is defined as the realization of electronic systems that are made using micro-scale electrical components. Recent technological improvements have allowed electronic devices to get smaller, but there has not been much improvement in battery technology. The energy density of commercial batteries has been shown to rapidly decrease with size, limiting their functionality in microelectronic systems. Developmental work from various research institutions has resulted in micro-batteries that are infeasible for commercial use, but these batteries are quite expensive, and utilize a two-dimensional electrode structure, which limits energy density. The utilization of a three-dimensional electrode structure could significantly improve the energy density of micro-batteries. The goal of this project was to develop a fully functioning, low cost, high energy density micro-battery utilizing a three-dimensional electrode structure to increase energy density. To accomplish this goal, the team established the following objectives:

1. Develop an effective packaging technique that could hermetically seal the battery
2. Develop and test a polymer gel electrolyte separator capable of being injected into the battery
3. Develop a process to build the battery that would result in successful operation
4. Perform a series of tests on the battery to measure charge capacity, energy density, and cycle life

The team used Pyrex glass tubes purchased from Pegasus Glass to house the internal materials of the battery. The internal components were sealed inside the glass housing using metal rod current collectors and a Loctite epoxy adhesive, which was applied to the current collector and glass junction to create a hermetic seal. The tips of the aluminum dowel pins were

lightly sanded and the copper rods were precision machined to ensure an interference fit between the current collector and the glass tube. The team then determined the quality of the sealing process by sealing sample of lithium metal in a glass housing using the process mentioned above, and then submerged the glass tube in water.

The internal battery components consisted of a LiCoO₂ cathode, a graphite anode, and a PMMA-PVDF polymer gel electrolyte (PGE) separator. A Teflon Swagelok Cell was used to test the charge and discharge capacity of the PGE separator as well as its cycle life. Once the active and inactive materials had been processed, the final processing and sealing of the battery was conducted in an argon glove box to avoid contamination from oxygen and water. Finally, an ARBIN electrochemical testing system was used to test the performance of the fully assembled batteries.

The PGE was tested using charging currents of C/10, C/5 and C/1 and which were determined based on the theoretical capacity of the PGE using the following formula,

$$C = \frac{\left(m_{Cathode} * 0.8 * 137 \frac{mAh}{g}\right)}{1000 \frac{mA}{A}} = Ah$$

$$Mass\ of\ Cathode = 0.0011\ g$$

Therefore, the charging currents were as follows:

$$\frac{C}{10} = 1.2056 \times 10^{-5}\ Amps \quad \frac{C}{5} = 2.4112 \times 10^{-5}\ Amps \quad \frac{C}{1} = 1.2056 \times 10^{-4}\ Amps$$

The results of electrochemical testing showed a charge – discharge capacity of approximately 80% - 90% (0.0964 mAh - 0.1085 mAh) of the theoretical capacity (0.1206 mAh). A decrease in capacity retention was observed after 30 cycles. These are expected results for a lithium anode battery since volume expansions and contractions during charging and discharging cause significant cracking and internal flaws in the anode, which eventually lead to cell failure.

Initial testing of battery performance showed that many cells suffered from short-circuiting. To correct this issue, a new method was developed of building the electrodes separately on their respective current collectors instead of stacking all of the internal battery components on top of each other. Additionally, a gap separator battery was developed that removed the PGE separator from the battery, and ensured that no short-circuiting could occur. The gap separator battery proved to be the most functional of the batteries developed, and produced a maximum charge capacity of approximately 0.243 mAh. The discharge capacity of the gap separator cells was 0.0694 mAh, which was quite small compared to the theoretical charge capacity, which was 0.6905 mAh. Additionally, the gap separator battery was able to charge and discharge approximately 3 times before the cell lost all appreciable charge capacity. This low discharge capacity was a common theme throughout battery testing and it was noted that the batteries had difficulty maintaining potential once charged. Testing of the micro-battery utilizing a PGE separator had minimal success, and it was determined that further development and testing was required in order to make a fully functioning battery.

Many challenges had to be overcome while completing this project. The small size of the batteries and components made processing each cell very difficult. There were major challenges assembling the cell as the glass housing was very brittle and applying too much stress caused them to break. Furthermore, inserting the active components into the glass battery housings proved to be very difficult, especially while working in the glove box, which limited dexterity.

Throughout this project, a significant amount of information was learned about the structure and chemistry requirements of a micro-battery, and significant progress was made in developing a micro-lithium ion battery using simple, low-cost methods. Several methods of building the battery were developed and marginal success was achieved at producing a battery

that could be charged and discharged. Overall, the experimental micro-lithium ion batteries that were produced had insufficient energy density and cycle life for marketability, and the following objectives and focuses were conceived in order for future work to have greater success:

1. Future batteries should utilize glass with thinner walls to reduce the amount of inactive materials used. Also the application of polymers for battery housings should be explored.
2. Future work should determine the optimal amount of epoxy needed to seal the cell to reduce the overall volume of the assembly, while maintaining a hermetic seal.
3. The issue leading to the batteries being unable to maintain their potential after charging needs to be addressed and solved. This issue was related to many of the batteries' issues including: poor electrode structure, improper adhesion between the electrodes and current collector, and insufficient saturation and gelling of the PGE separator.

1.0 Introduction

Electronics is defined as the arrangement of electrical components into integrated circuits, which provide a useful output. Electronics are used in information technology, telecommunication, visual and audio recording devices, sensors and many other applications. The electronics industry has undergone immense growth, and as electrical circuits have become more complex, their size, weight and power requirements have rapidly changed as well.

During World War 2, there was a need for smaller and lighter electrical equipment, which soldiers could easily carry and operate on the battlefield. These requirements are also important factors in the development of modern electrical devices. As engineers made gradual improvements in electrical technology, the resulting devices became smaller and more efficient. These smaller devices are described using the term, microelectronics.

Microelectronics is defined as the area of technology that is associated with the realization of electronic systems that are made using micro-scale electrical components. Due to the current trend of producing a number of circuits on a single chip, there is a need to increase the packing density of the electronic circuits. Along with increasing the packing density, there is a need to reduce the size and weight of the components, as well as to improve the efficiency and reliability of the microsystem.

In an effort to improve the packing density, many engineers are trying to supply their microcircuits using micro-batteries. According to King et al (2013) technological improvements have allowed electronic devices to get smaller, but there has not been much improvement in battery technology. The use of micro batteries in these microsystems could reduce the overall size and weight of the circuit as well as supply it with adequate voltage and current.

According to Lai et al. (2010), the energy density of commercial batteries rapidly decreases with size; reaching undesirable levels before volumes of interest ($< 0.1\text{cm}^2$) are reached. They also stated that this trend corresponds to a decreasing ratio of active materials to inactive materials; resulting in the battery being significantly larger than the connected microcircuit. In an effort to avoid this problem, researchers are developing micro-batteries. However, many of these micro-batteries are produced in research settings and are difficult and costly to manufacture.

The proceeding sections of this paper will present some prerequisite background information about batteries, discuss the methods we developed for creating micro-batteries, present and discuss the findings of our experimental trials, state the conclusions reached as a result of this project, and offer our recommendations for future continuation of this work.

2.0 Background

In this section, background information about batteries will be presented, including an overview of battery operation, a brief history of the development of battery technology, details on inactive and active battery materials, safety concerns, and finally the current state of micro-battery research, and the research niche of this project.

2.1 Overview

There are many different types of batteries, but they all function using the same concept. A battery is a device that stores energy as chemical energy and releases this energy in the form of electricity. A typical battery consists of three main components: the anode, the cathode and the electrolyte. The anode is the negative terminal, the cathode is the positive terminal, and the electrolyte is a chemical that separates the two terminals.

During discharge, the battery generates positive ions and electrons at the anode. As seen in Figure 1, the positive ions flow through the electrolyte to the positive electrode while the electrons flow through the external circuit towards the cathode, causing the light bulb to illuminate. If the battery is disposable, it will produce electricity until it runs out of reactants. These batteries only work in one direction, that is, they can only convert chemical energy into electricity. There are batteries, however, in which the reaction can be reversed. Such batteries known as rechargeable batteries, and are designed so that electrical energy from an external source can be supplied to the battery. This external energy reverses the operation of the battery and restores the battery's charge. The most common rechargeable batteries on the market today are lithium-ion (Li-ion) batteries, although nickel-metal hydride (NiMH) and nickel-cadmium (NiCd) batteries were also once very prevalent.

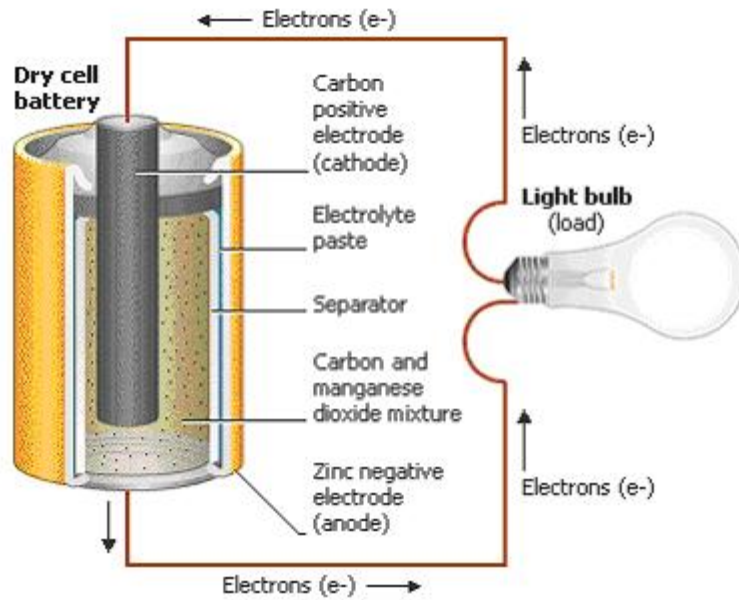


Figure 1: Diagram of a battery circuit

A Lithium ion (Li-ion) battery is a type of rechargeable battery that utilizes the transfer of lithium ions between a lithium based positive electrode and a negative electrode. Several variations of Li-ion battery exist that implement different active materials in response to the requirements of certain applications. These batteries are used in many areas including cellular phones, laptop computers, global positioning systems, and electric vehicles. According to Mckissock et al (2009), Li-ion batteries are also used in aerospace applications, including satellite systems, astronaut spacesuits, and lunar and planetary rovers. Carnegie et al (2013), stated that Li-ion batteries are characterized by their high energy density, low standby losses, and cycling tolerance. These properties make these cells an ideal energy source for many mobile and weight sensitive applications.

Tarascon and Armand (2001) stated that lithium is a suitable material for batteries because of its low atomic number and its high electrode potential. The combination of these two properties results in a much greater energy density when compared to other battery technologies.

Figure 2 compares the energy density by weight and volume of various types of batteries. It can be seen from the figure that Li-ion batteries have a much higher energy density than previous technologies.

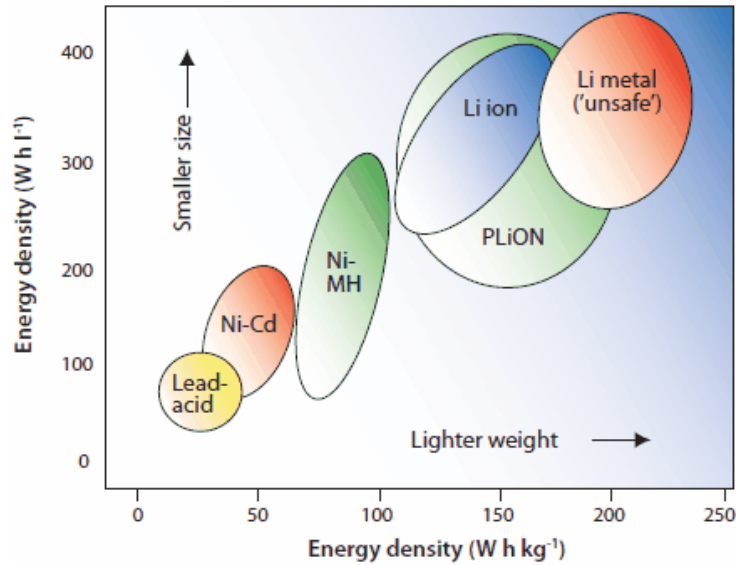


Figure 2: Energy densities of various batteries types

2.2 History of Battery Technology Development

According to Buchmann (2001), one of the most remarkable and novel discoveries over the past 400 years has been electricity. He stated that the first practical use of electricity came in the late 1800s, during an exposition in Paris in which a bridge over the river Seine was illuminated by approximately 250,000 light bulbs.

2.2.1 Early Batteries

Scientists and historians believe that the use of electricity dates back farther. According to Downs and Meyerhoff (2000), workers who were building a railway near Baghdad in 1936 discovered what seemed to be a prehistoric battery. This battery is known as a Parthian battery, which dates back to the Parthian period; meaning that this battery is over 2000 years old. The

battery consisted of a clay jar that was filled with a vinegar solution. An iron rod surrounded by a copper cylinder was inserted into this vinegar solution. The device produced 1.1 – 2 volts of electricity and a diagram of the battery is shown in the figure below.

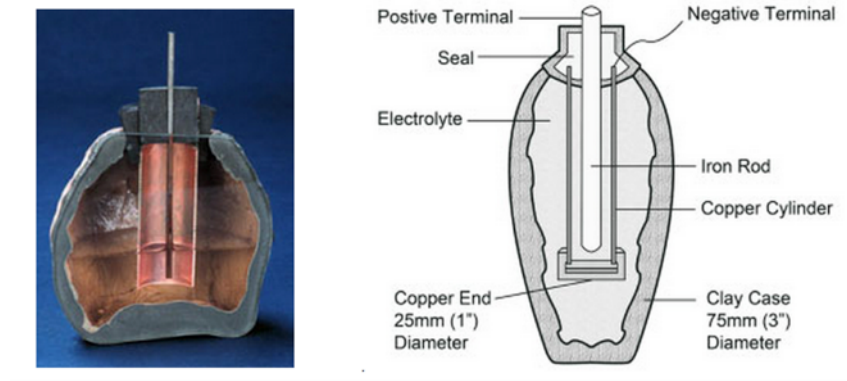


Figure 3: A Parthian battery

Alessandro Volta (1745-1827) discovered in 1800 that certain fluids would generate a continuous flow of electrical power when they are combined with a pair of dissimilar metals. This discovery led to the invention of the first voltaic cell, more commonly known as the *battery*. He also discovered that the voltage would increase when these voltaic cells were connected in series. The figure below shows the configuration of Volta's battery.

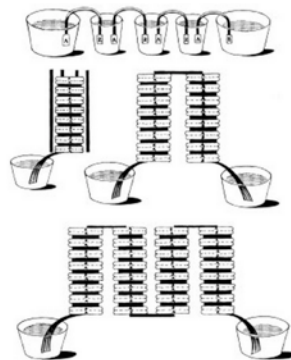


Figure 4: Configuration of Volta's battery

Buchmann (2001) stated that France was one of the first nations to officially recognize Volta's discoveries. He then stated that France, at the time, was approaching the height of scientific advancements and the French welcomed any new ideas. He added that Volta spoke at

the Institute of France in a series of lectures, which Napoleon Bonaparte attended. Napoleon helped with the experiments, which included drawing sparks from the battery, melting a steel wire, discharging an electric pistol and decomposing water into its elements.

After many successful experiments and the discovery of the voltaic cell, interest in galvanic electricity became widespread. Sir Humphry Davy (1778–1829), inventor of the miner's safety lamp, made new discoveries when he installed the largest and most powerful electric battery into the vaults of the Royal Institution. He connected the battery to charcoal electrodes and produced the first electric light.

In 1802, Dr. William Cruickshank (1727 – 1810) designed the first electric battery that could be mass-produced. Cruickshank gathered square sheets of copper with an equal amount of zinc sheets. He placed these sheets in a long rectangular, wooden box and soldered them together. Grooves in the box held the metal plates in position. Lastly he filled the sealed box with an electrolyte of brine, or diluted acid, resembling the wet cell battery that still exists today.

2.2.2 Rechargeable Batteries

In 1836 John F. Daniell (1790 – 1845), an English chemist, developed an improved battery that produced a steadier current than Volta's device. Until then, all batteries were primary, meaning that they could not be recharged. In 1859 the French physician, Gaston Planté (1834 -1889), invented the first rechargeable battery, which used lead and acid, a system that is still used today.

In 1899, Waldmar Jungner (1869 – 1924) of Sweden invented the nickel-cadmium (NiCd) battery, which used nickel for the positive electrode and cadmium for the negative electrode. Two years later, Thomas Edison (1847 – 1931) produced an alternative design by replacing cadmium with iron. Due to high material costs, the practical applications of the nickel-

cadmium and nickel-iron batteries were limited. As a result of major improvements made by Shlecht and Ackermann, NiCd cells gained new attention. These improvements resulted in higher load currents and improved longevity. A breakthrough came in 1947 when Georg Neumann (1898 – 1976) succeeded in completely sealing the nickel-cadmium cell.

According to Buchmann (2001), in the 1980s and 1990s scientists extensively studied nickel-based chemistries. He also stated that NiCd cells were hazardous to the environment and some European countries restricted the use of this chemistry and asked for a switch to nickel metal hydride (NiMH). Many scientists said, according to Buchmann, that the NiMH chemistry was an interim step to the Li-ion cell and most of the resulting research focused on improving lithium-ion batteries. See Appendix A for a summary of the major historical developments in battery technology.

2.3 Battery Packaging

Batteries consist of both inactive and active materials, and both are vital for operation. Inactive battery materials include any vital component of the battery that does not take part in the electrochemical reactions that create current and potential in the battery system. Inactive materials include the battery outer packaging and sealing, the current collectors, and the electrolyte. Active battery materials include the anode and cathode, which physically take part in the production and storage of lithium ions and electrons.

Battery packaging is an important component that prevents contamination of the electrochemical reaction and provides structure and shielding for the battery. Over the years, manufacturers have developed various techniques of packaging batteries. These techniques have

been developed to fulfill various requirements of performance, size and weight and each technique has its associated advantages and disadvantages.

2.3.1 Cylindrical Cell

Currently, the cylindrical cell is one of the most widely used packaging styles for primary and secondary batteries due to its ease for manufacturing. These batteries have good mechanical stability, that is, they can withstand high internal pressures without deforming.

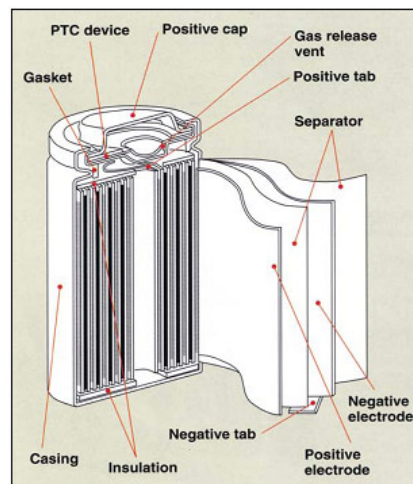


Figure 5: Cross section of a Li-ion cylindrical cell

Nickel-cadmium (NiCd) batteries display the largest variety of cell configurations. Scientist used some of these configurations to develop the nickel-metal-hydride (NiMH) battery. Despite the many established configurations of cylindrical cells, scientists established a unique configuration for the Li-ion battery. The 18650 illustrated in Figure 6 remains one of the most popular cell packages. The 18650 is a Li-ion cell that is housed in a metallic cylinder which measures 18mm in diameter and 65mm in length.



Figure 6: Popular 18650 li-ion cell

According to Battery University, in 2013 manufacturers produced 2.55 billion 18650 cells initially with a 2.2Ah capacity but now, most cells have a capacity of 2.8Ah. Some newer 18650 Energy Cells are 3.1Ah and scientists predict that the capacity will grow to 3.4Ah by 2017. Cell manufacturers are striving to develop a cell that is 3.9Ah, which they hope will be the same cost as cells of lower capacities.

2.3.2 Button Cells

The button cell, also known as the coin cell, had a compact design, which was suitable for powering portable devices of the 1980s. Scientist achieved higher voltages by stacking these cells into a tube thereby enabling these batteries to power cordless telephones, medical devices and security wands at airports.

Although small and inexpensive to build, the stacked button cell became undesirable and was replaced by more conventional battery formats. One drawback of the button cell is that the cell swelled if charged too rapidly. Button cells have no safety vent and can only be charged during a 10- to 16-hour period; however, newer designs claim to have a rapid charge capability.

Most button cells in use today are non-rechargeable and are found in medical implants, watches, hearing aids, car keys and memory backup. Figure 7 illustrates the button cells with an

accompanying cross section. It is recommended that these cells be kept out of reach of children as swallowing the cell can cause serious health problems.

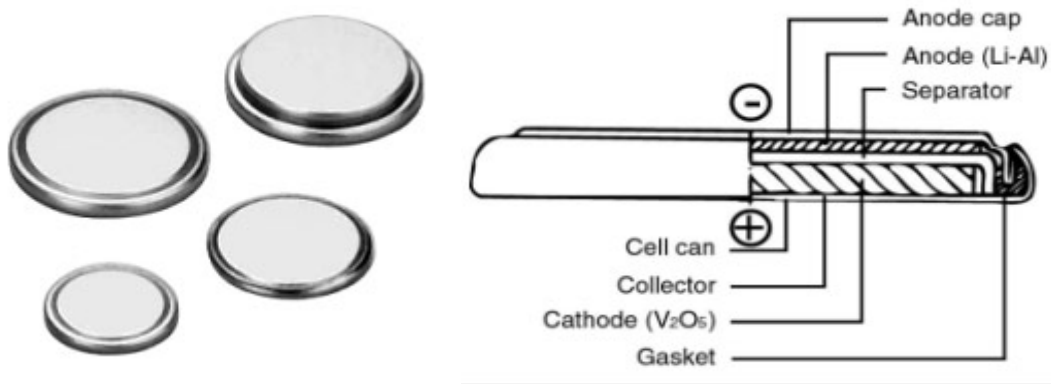


Figure 7: Button cells

2.3.3 Prismatic Cells

Introduced in the early 1990s, the modern prismatic cell satisfies the demand for thinner sizes. These cells are housed in elegant packages, which resemble a box of chewing gum or a small chocolate bar and make optimal use of space by using the layered approach. These cells are predominantly found in mobile phones, tablets and low-profile laptops and range from 800mAh to 4,000mAh. No universal format exists and each manufacturer designs its own unique battery format.

Prismatic cells are also available in larger models, which are typically packaged in welded aluminum housings. These cells deliver capacities of 20 to 30Ah and are primarily used for electric powertrains in hybrid and electric vehicles.

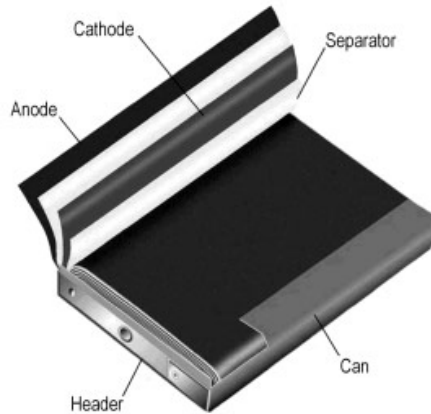


Figure 8: Prismatic cell

The prismatic cell requires a slightly thicker wall to compensate for a decreased mechanical stability compared to that the cylindrical design. Some swelling due to gas buildup is normal, however, one should discontinue using the battery if the distortion becomes so large that it presses against the battery compartment.

2.3.4 Pouch Cell

In 1995 the pouch cell revolutionized the battery industry with a radical new design. Instead of using a metallic cylinder, manufacturers welded conductive foil-tabs to the electrodes and brought these tabs to the outside while fully sealing the internal components of the cell.

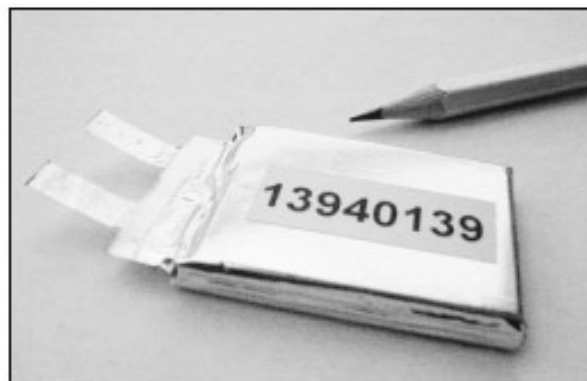


Figure 9: Pouch cell

The pouch cell makes the most efficient use of space and achieves a 90–95 percent packaging efficiency, the highest among battery packs. Eliminating the metal enclosure reduces

weight but the cell does need some support in the battery compartment. These pouch packs are used in consumer, military and automotive applications.

Pouch packs are commonly Li-polymer and serve as power cells, which deliver high current. The capacity of these cells is lower than that of the Li-ion cylindrical cell but the pouch pack is more durable than the flat-cell. Manufacturers state that slight swelling of the pack over 500 cycles is normal and that the battery compartment must be large enough to accommodate this expansion.

Extreme swelling is a concern but battery manufacturers insist that these batteries do not generate excess gases. According to Battery University, most swelling can be blamed on improper manufacturing and users of pouch packs have reported few swelling incidents. The pressure created can crack the battery cover and in some cases, it can break the display and electronic circuit boards. Manufacturers say that an inflated cell is safe but discontinue using the battery and do not puncture it.

2.4 Current Collectors

One of the areas of research that scientists have focused on is the development of current collectors. These collectors are typically highly conductive materials that facilitate the flow of electrons in batteries. These current collectors are usually metals or metal alloys, which have high electrical conductivity. The figure below shows a simple battery configuration, which displays the placement of current collectors in relation to the cathode, anode, and separator.

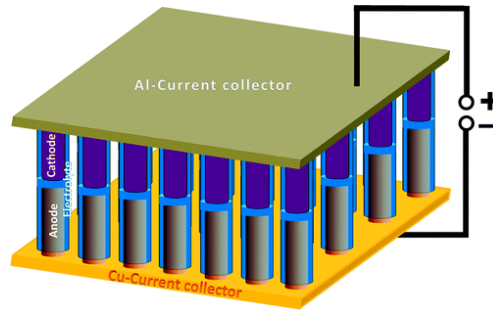


Figure 10: Simple battery configuration which highlights the placement of the current collectors

For most commercial Li-ion batteries the current collector of the cathode is aluminum and that of the anode is copper. Whitehead and Schreiber (2005) stated that these current collector materials are ideal because they have high electron conductivity, are readily available in many forms, and are price effective. The table below displays the relative conductivity per unit volume, mass, and price of various materials.

Table 1: Comparison of various current collector materials

Material	Relative conductivity per unit volume	Relative conductivity per unit mass	Relative conductivity per unit cost
Ag	1.05	0.9	0.01
Cu	1	1	1
Au	0.7	0.33	0.00008
Al	0.4	1.3	2
Mo	0.31	0.27	0.01 ^a
W	0.29	0.13	0.02
Zn	0.28	0.36	0.8
Ni	0.24	0.25	0.05
Fe	0.17	0.20	2 ^a
Pt	0.16	0.067	0.000008
Cr	0.13	0.16	0.05
Ta	0.13	0.072	0.001 ^a
304SS	0.1	0.1	0.1 ^a
316SS	0.1	0.1	0.07 ^a
Ti	0.040	0.079	0.02 ^a
SiC	0.012	0.032	0.001
Mn	0.009	0.01	0.01
C pyrolytic graphite	~0.007	~0.03	— ^b
C graphite	~0.0003	~0.0012	~0.0005
C black	~0.00001	~0.00004	~0.00002

^a Pure scrap prices.
^b No bulk prices available.

From the table, it is seen that aluminum and copper have some of the highest electron conductivities per unit mass and volume. Gold and silver have higher conductivities per unit

volume, but aluminum and copper have the highest electron conductivity per unit price. These characteristics make copper and aluminum suitable for commercial use.

Some important factors to consider when selecting current collectors are corrosion and fatigue. According to Braithwaite et al (1999), aluminum environmental degradation occurs most frequently in the form of pit corrosion while in copper, cracking is the most prominent form of degradation.

Braithwaite and researchers at the Sandia National Laboratories showed that in aluminum, pit corrosion occurs because the positively charged electrode has a high oxidizing potential. Aluminum oxide pits or mounds form on the surface of the aluminum, decreasing the structural integrity of the aluminum current collector.

They showed that the copper current collector experienced cracking when metallurgical conditions such as work-hardened copper or copper with large grain sizes existed. The work-hardened copper cracked during cycling because of the increased inner strains within the copper. Large grain sizes lead to lower strength and fracture toughness, which made the material more susceptible to cracking.

2.5 Electrodes

Along with developing ideal current collectors, scientists are also developing suitable electrodes. An electrode is a conductor that passes a current from one medium to another. In batteries, there are two electrodes, the anode and the cathode. At the anode, electrons leave the cell and oxidation occurs. Meanwhile, electrons enter the cell through the cathode and reduction takes place. Electrodes are considered active materials because they are involved in the electrochemical reactions that cause the battery to function.

2.5.1 Anodes

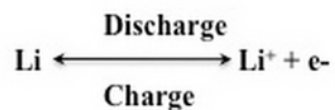
The anode is the negative electrode of a primary cell and is always associated with the oxidation or the release of electrons into the external circuit. In a rechargeable cell, the anode is the negative pole during discharging and the positive pole during charging.

Lithium Anode

According to an article from Cornell University (2014), the effective development of a high energy density cell requires the use of high-energy capacity materials. The article stated that in order to achieve high energy densities, alkali metals are ideal. The most promising rechargeable batteries, according to the article, use lithium anodes, as lithium is the easiest to handle, the lightest, and the most electropositive of all the alkali metals. The article stated that lithium batteries have the highest voltage and energy density of all other rechargeable batteries and are favored in applications related to portable appliances where low weight and small volume are the major constraints. There are several advantages of using lithium anodes as they are:

- Good reducing agents
- Highly electropositive
- High capacity and energy density components
- Good conducting agents
- High mechanical stability components
- Easy to fabricate

The essential equation for the metallic lithium anode is as follows



Despite the benefits of using lithium anodes, there are difficulties with implementing them in rechargeable batteries. According to the article (2014), one issue is that Lithium metal tends to deposit as a dendrite or mossy structure during charge, and the disordered metallic deposit results in a poor charge in the battery. The article stated that this happens because Lithium metal often decomposes the electrolyte and can seep into the separator; eventually causing an internal short-circuit. These lithium metal cells also had the tendency for thermal runaway, which is a situation where an increase in temperature changes conditions in a way that causes a further increase in temperature. The temperature in these cells would quickly rise to the melting point of the metallic lithium and cause a violent reaction. The article stated that due to the hazardous reactions of lithium and the electrolyte, other safer anodes have been developed.

Silicon Anode

Chan et al. (2007) stated that there is a high interest in developing high energy density batteries for various purposes, a similar statement to that made in the article from Cornell University. They stated that silicon is an attractive anode material for lithium batteries because it has a low discharge potential and it has the highest known theoretical charge capacity. They also added that even though this charge capacity is more than ten times higher than that of existing graphite anodes and much larger than that of various nitride and oxide materials, silicon anodes have limited applications because their volume changes by up to 400% due to insertion and extraction of lithium ions, which leads to pulverization and capacity fading.

Carbon Anode Materials

According to the article from Cornell University (2014), the use of compounds containing carbon which allow the intercalation of Lithium are the most suitable candidates for anode materials. The widespread use of such compounds has led to the development of the

popularly known Li-ion Battery. The article also stated that most carbon varieties including graphite are becoming more attractive candidates for rechargeable lithium battery anodes because they can accommodate lithium reversibly, offer high capacity, have good electronic conductivity and they have low electrochemical potential. According to the article, the cost, availability, performance and electrochemical potential of carbon-based materials are all acceptable and even preferable when compared to lithium metal anodes. The article then stated that there is no significant swelling or stack pressure generated by the carbon electrodes during prolonged cycling and therefore, Li-ion cells can be constructed as flat or prismatic cells with thin-walled cases or they can be constructed in any other cell configurations. The shortcomings on the deployment of different types of anode materials are displayed in the table below.

Table 2: Remarks on various anode materials

Anode Material	Notes
Lithium	Dendrite growth, expensive, toxic
Carbon	Irreversible capacity loss
Tin	Inclusion of solid electrolyte phase in the electrode
Atco	Complicated lithium uptake/removal
M-M Alloy	Larger volume changes (mechanical decrepitating)
Ternary Metal Vanadates	Arguable Li diffusion mechanism
Metalloids	Moisture sensitive

2.5.2 Cathodes

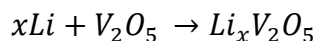
The cathode is the positive electrode, which attracts positively charged ions. It is associated with the reduction or the gaining of electrons from the circuit. It then releases these electrons, which move through the external circuit towards the anode. In a rechargeable cell, the cathode is the positive terminal during discharge and the negative terminal during charging.

According to the article from Cornell University (2014), research on cathodes for Li-ion cells have been directed towards crystalline metal oxide based materials. Fergus (2010) made a

similar statement by saying that cathode materials are usually oxides of transitional metals, which undergoes oxidation to higher valences. Whittingham (2004) also made a similar statement, however, he added that in the past, layered oxides were not studied because scientists thought that these oxides would not readily remove lithium ions.

Early Studies of Layered Oxides

According to Whittingham (2004), Vanadium pentoxide (V_2O_5) and molybdenum trioxide (MoO_3) were two of the earliest studied oxides. He also stated that molybdenum trioxide readily reacted with lithium, but due to its low rate of reaction this compound was of little interest. Vanadium pentoxide, on the other hand, has been studied for over thirty years according to Whittingham. He also states that the compound has a layered structure with weak vanadium-oxygen bonds between layers and is known to react by the following intercalation mechanism:



Lithium Cobalt Oxide ($LiCoO_2$)

Whittingham (2004) stated that nickel cobalt oxide had a structure similar to that of the dichalcogenides and after many experiments, lithium can be electrochemically removed from this compound, which made it a viable cathode material. He also stated that SONY combined a $LiCoO_2$ cathode with a carbon anode to create the first successful Li-ion battery. Fergus (2010) added that nickel cobalt oxide is the most commonly used cathode material today due to how easily lithium ions can be inserted and removed. He stated that even though $LiCoO_2$ is a successful cathode material, scientists are developing alternate cathodes in order to lower costs and improve stability. He added that cobalt is not as readily available as other transitional metals; making it more expensive. He then stated that $LiCoO_2$ is not as stable as other potential cathodes as it can degrade or fail over time. Whittingham also discussed the limitations of using $LiCoO_2$

and he stated that another type of cathode with a similar structure to that of LiCoO_2 must be developed.

Lithium Nickel Oxide (LiNiO_2)

Fergus (2010) stated that lithium nickel oxide has a similar structure to that of LiCoO_2 but is less expensive and has a higher energy density, Despite these positive characteristics, LiNiO_2 is less stable and is less ordered. Whittingham (2004) added to what Fergus said by stating that the nickel ions occupy spaces in the lithium layer; impeding the flow of free lithium ions and reducing the power capability of the cell. Secondly he stated that compounds with a low lithium content, such as LiNiO_2 , tend to be unstable due to high oxygen partial pressure and are dangerous if they come into contact with organic solvents. Both Fergus and Whittingham stated that adding cobalt to the compound will improve the ordering, this is, the nickel ions will occupy the nickel/cobalt plane instead of the lithium plane. This reorganization forms a $\text{LiNi}_{1-x}\text{Co}_x\text{O}_2$ structure, which consists of mostly nickel and as a result, scientists and engineers have been able to take advantage of the low cost and high energy density of nickel. Please see Appendix C for more information about different types of cathodes.

2.5.3 Three-Dimensional Electrodes

As stated earlier, improvements in micro-battery technology have lagged behind the improvements in microelectronics. According to Arthur et al. (2011), the size of these microelectronic devices are determined by the size of the power supply and integrating these power sources within the device is not possible due to the size of the devices.

Arthur et al. (2011) stated that a key consideration when developing microelectronics especially for integrated power is the footprint area of the device. They stated that traditional 2D battery designs require large footprint areas to achieve high capacities. This space requirement is

particularly evident with thin film micro batteries, which have limited capacities. Arthur et al (2011) also stated that making the electrodes thicker is not possible because the additional weight will compromise the mechanical integrity of the cell.

3D battery architectures take advantage of the third dimension, height, to increase the amount of electrode material within the footprint area; resulting in significantly higher capacities. According to Arthur et al. (2011), the field the 3D batteries are expected to significantly improve during the next few years due to major advances in synthesis techniques. Due to the 3D structure, the cell will be able to rapidly charge and discharge, however, this structure can lead to unwanted side reactions in the electrodes. Furthermore according to Arthur et al. (2011), one of the main challenges remaining in the field the 3D batteries is the integration of complementary electrode, that is, if one starts with a high surface area 3D anode, integrating the cathode is a significant challenge. Successfully incorporating 3D electrodes into a cell greatly depends on the structural integrity of the electrolyte as excess stress in the cell can cause irreversible damage to the electrolyte.

2.6 Electrolytes and Separators

The purpose of the electrolyte and separator in a battery is to aid in the transfer of ions between the anode and cathode. Separators act as a barrier between the electrodes in order to prevent short-circuiting, while allowing efficient ion transfer through the battery. The electrolyte aids in this process, allowing for low resistance ionic transfer (Bates, 2012).

2.6.1 Electrolytes

In order to provide low resistant transport, electrolytes are typically a solution of ionic salt in a non-conductive organic solvent. For lithium ion batteries, common electrolytes are

lithium salts such as LiPF_6 , LiBF_4 , and LiClO_4 dissolved in ethylene carbonate (EC), dimethyl carbonate (DMC), or diethyl carbonate (DC) (Xu, 2004). For this project, a solution of LiPF_6 in an EC/DC/DMC mixture was utilized due to its availability and compatibility with the LiCoO_2 cathode material.

2.6.2 Separators

There are several types of separator mechanisms utilized in lithium ion batteries including solid, and polymer gel electrolyte (PGE) separators, as well as systems where a physical gap between the electrodes acts as an effective separator. Separators must be chemically inert to the other active materials in the battery to prevent contamination of the electrochemical reactions. Additionally, whether a physical separator is utilized or a gap between the electrodes, the separator mechanism must be very thin, in order to maximize ionic transport efficiency (Orendorff, 2012).

Solid Separators

Solid separator systems are typically made of single or multi-layer polymer sheets. In small cell commercial batteries, polyethylene or polypropylene sheets are typically used due to their low cost, high porosity (~40%), low ionic resistivity, and chemical inertness. These materials can also be manufactured in very thin sheets (~25 μm), while still providing the structural integrity necessary for holding potential above 4 volts, and long cycle life (Orendorff, 2012).

Polymer Gel Electrolytes

Polymer gel electrolytes (PGE's) are a developing technology with the potential to improve ionic conductivity, while maintaining thermal resistance and reducing the safety hazards of a typical solid separator – liquid electrolyte system (Zhang, 2014). PGE's are a unique

combination of the separator and electrolyte system, where the gel base absorbs the liquid electrolyte and simultaneously acts as the separator and electrolyte for the battery.

The PGE developed for this project was based on the work of H.P. Zhang et al, “A novel sandwiched membrane as polymer electrolyte for lithium ion battery” (Zhang, 2007). This paper outlines the development of a PGE with 3-layer structure of poly (vinyl difluoroethylene) (PVDF) and poly (methyl methacrylate) (PMMA). The design proposed by the paper consisted of 2 outer layers of PVDF surrounding a layer of PMMA in a weight ratio of 0.5:1:0.5. In this design, the inner PMMA layer acted as a sponge, which easily absorbed the liquid electrolyte and formed a gel, while the PVDF outer layers were highly porous and gave mechanical strength to the PGE (Zhang, 2007).

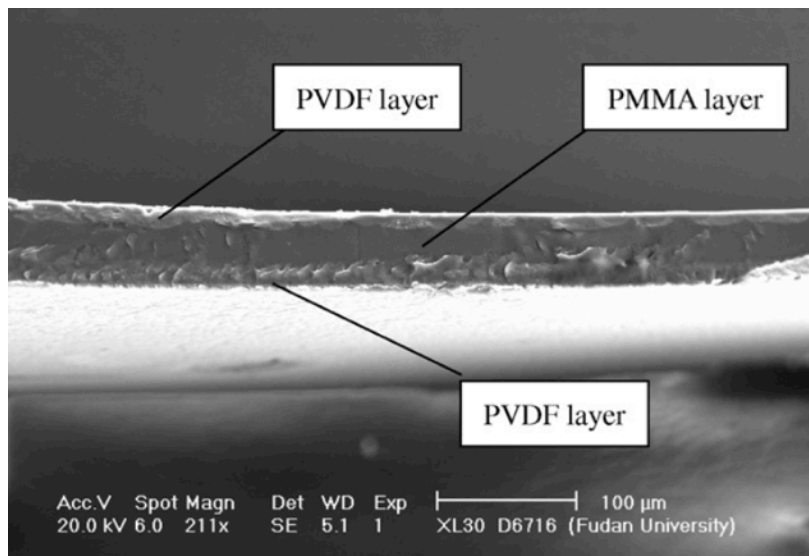


Figure 11: The three layer sandwiched PGE developed by H.P. Zhang et al (Zhang, 2007)

PMMA has a melting point of about 180 °C, which is much higher than the polyethylene (PE) used in commercial solid separators, which has a melting point of just 120 °C. This higher heat durability of the PGE prevents the pores of the separator from closing at high temperatures and leads to improved safety of the battery. PVDF also shows greater mechanical strength than PE and does not dissolve in the liquid electrolyte, improving battery performance. Additionally,

this PGE has been shown to increase the evaporation temperature of the electrolyte to 160 °C, allowing for improved cycle life and reducing the likelihood of the liquid electrolyte reacting with electrode material. Various structures of the PGE have been studied, including layered and homogenous systems (Zhang, 2007).

Physical Gap Separators

A final separator method is using a gap between the electrodes instead of any physical separator material. This method is not widely studied due to its impracticality in a commercial battery, but has been shown to be effective in the laboratory setting. Having a physical space between the electrodes and filling that space with liquid electrolyte accomplishes the objective of any other separator, in that ions can freely flow between the electrodes while avoiding short-circuiting. However, this method is not favored and is not utilized in commercial batteries due to the difficulty of creating the same spacing between electrodes that is possible when using a physical separator.

2.7 Safety Concerns

Despite the revolutionary breakthroughs in active material technology, Li-ion cells have several safety concerns. Capozzo et al (2006), stated that there are several factors that can cause a Li-ion battery to fail. Poor quality control during the manufacturing process is one such factor. During processing, it is essential to prevent microscopic metallic fragments from contaminating the electrolyte. If these fragments breach the electrolyte, a short-circuit can occur.

They also stated that another factor that can cause failure is external exposure to heat. This exposure includes leaving the battery in sun or close to a heat source. The additional heat causes the cathode to breakdown; releasing oxygen into the sealed battery. This accumulation of

oxygen increases the pressure inside the battery and generates more heat. Due to the increase in pressure, the battery could potentially explode. Furthermore, as the chemical reaction inside the battery produces its own heat, there is always a possibility that the battery will combust and this issue is exacerbated if the cell is exposed to heat.

Capozzo et al (2006) stated that the chemicals in batteries are hazardous after the cell has malfunctioned. According to Hammel et al (1995), previous testing has shown that lithium ion batteries contain chemicals that break down into toxins, which can seep out of the battery. If a battery were to overheat or combust, the personnel involved in the clean up could potentially be exposed to hazardous toxins. Capozzo et al (2006) lastly stated that the average consumer is unaware of the hazards associated with these batteries and the precautions to take once the battery fails.

2.7.1 Failure Mitigation

According to Capozzo et al (2006), there have been new improvements in battery technology that will mitigate failures. As the majority of failures occur due to high temperatures, many manufacturers have installed two switches on their batteries, which will activate at a specified temperature. They stated that the first switch will open at approximately 70°C; preventing the battery from charging and will reset once the battery cools down. This switch allows the battery to operate at safe temperature and prevents the battery from overheating. The other switch will permanently shut down the battery if the temperature exceeds 90°C. After this switch is activated, the battery will no longer be able to charge or discharge; not even if the battery cools down. This switch provides protection in extreme situations in which the temperature of battery continues to increase after the first switch has already been activated. For more information about the safety of Li-ion batteries, please see Appendix D.

2.8 Current State of Micro-Battery Technology

There have been few improvements in the field of micro-battery technology in comparison to the recent breakthroughs in microelectronics. Current research on micro-battery technology is scarce, but several processing methods have been developed to create micro-batteries of various scales and designs. These techniques will be described in greater detail in this section.

2.8.1 Commercial Micro-Batteries

In October 2014, Panasonic developed and commercialized the smallest pin shaped battery, which was 20 mm in length and 3.5mm in diameter. Representatives from the company stated that the cell had a capacity of 13mAh and had a weight of 0.6g. Along with being the smallest cylindrical shaped rechargeable Li-ion battery, this battery features the high reliability and high output required for near field communications (NFC) applications. This cell is also suitable for powering wearable devices, which are anticipated to be the next wave of mobile devices after smartphones. Mass production and shipping are planned to begin in February 2015, with a monthly production of one hundred thousand units.

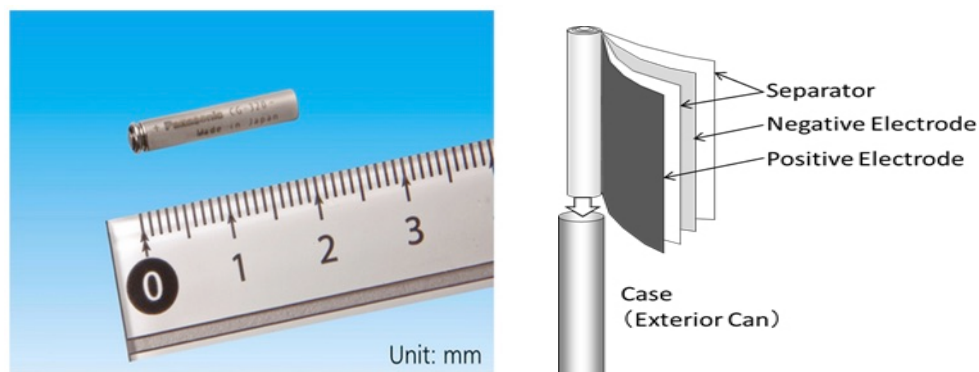


Figure 12: Panasonic pin battery

Panasonic has also developed a coin shaped Niobium-Lithium (NBL) rechargeable micro-battery. This cell is smaller than their pin shaped cell; measuring 4.8mm in diameter and

1.5mm in height. The cell has a capacity of 1mAh and is excellent at withstanding over-discharging and over-charging, it has a low self-discharge rate, it is ideal for new technology using low voltage integrated circuits (IC's) and it is suitable for backing up memory data in mobile telephones, pagers and other small communication devices.



Figure 13: Panasonic NBL micro-battery

Panasonic developed a manganese dioxide coin battery, called the CR1025, which measures 10mm in diameter and 2.5mm in height. Unlike the pin cell and the NBL micro-battery, this cell is non rechargeable but it has a capacity of 30mAh. This cell is suitable for powering watches, hearing aids and small medical devices.



Figure 14: Panasonic CR1025 coin battery

2.8.2 First 3-D Rechargeable Li Ion Micro-battery

In 2005, researchers at Tel Aviv University produced the first 3-D rechargeable Li-Ion battery, which was on the order of cubic millimeters. They utilized a perforated substrate to build the battery using a Molybdenum Sulfide cathode with a Ni current collector, a polymer

electrolyte, and a lithiated graphite anode, which also acted as the anode current collector. The substrate was 13mm in diameter and 0.5 mm thick, with 50-micrometer diameter hexagonal micro channels (Golodnitsky et al, 2006). A schematic of the substrate can be seen below in Figure 15.

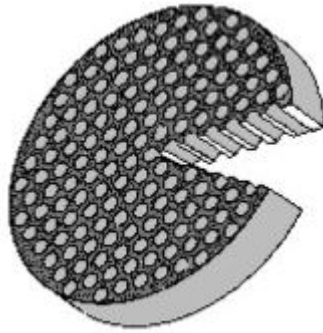


Figure 15: Substrate schematic

The battery showed significant capacity increases in comparison to typical 2-D batteries at high cycles. Figure 16 below illustrates the significant improvement. This achievement can be attributed to the increase in surface area due to the micro-channels in the substrate (Golodnitsky et al, 2006).

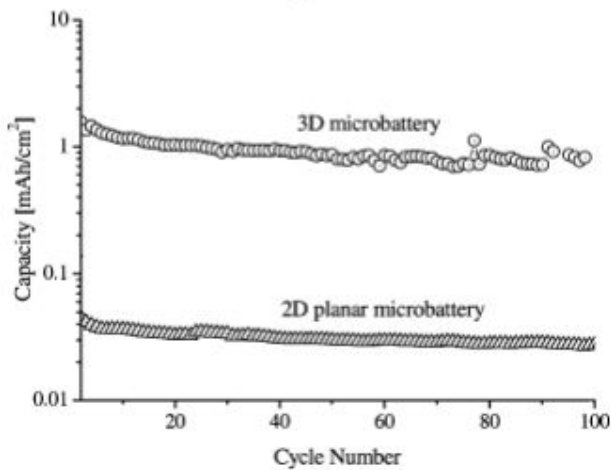


Figure 16: Improvements of 3D electrode micro-battery capacity

2.8.3 3D Inter-digitated Li-Ion Micro-Battery Architectures (Sun)

Researchers at the University of Illinois have 3D printed an inter-digitated Li-ion micro-battery using advanced processing methods. They printed gold current collectors onto a glass substrate using a combination of lithographic patterning and e-beam deposition. The spacing between the positively and negatively charged current collectors is 50 micrometers (μm). Then using a 3-axis micro-positioning stage, the scientists precisely printed the cathode and anode (LTO and LFP) onto the current collectors in an inter-digitated fashion. The composition and rheology of each ink is optimized to ensure that reliable flow occurs through the $30\mu\text{m}$ diameter nozzles, to promote adhesion between the printed features, and to provide the structural integrity needed to withstand drying and sintering without delamination or distortion. Once the printing process was complete, they housed the battery inside a thin layer of Poly(methyl methacrylate) (PMMA). The researchers then filled the assembly with liquid electrolyte and sealed it with Polydimethylsiloxane (PDMS) gel. The process of producing this battery is illustrated in Figure 17 below. The battery produced a capacity of $1.2\text{mAh}/\text{cm}^2$, but did not exhibit long-term cycle life due to a lack of hermeticity. They mentioned that effectively packaging micro-batteries ($<10\text{mm}^3$) is very challenging and that a few examples of stable micro-battery packaging have been reported.

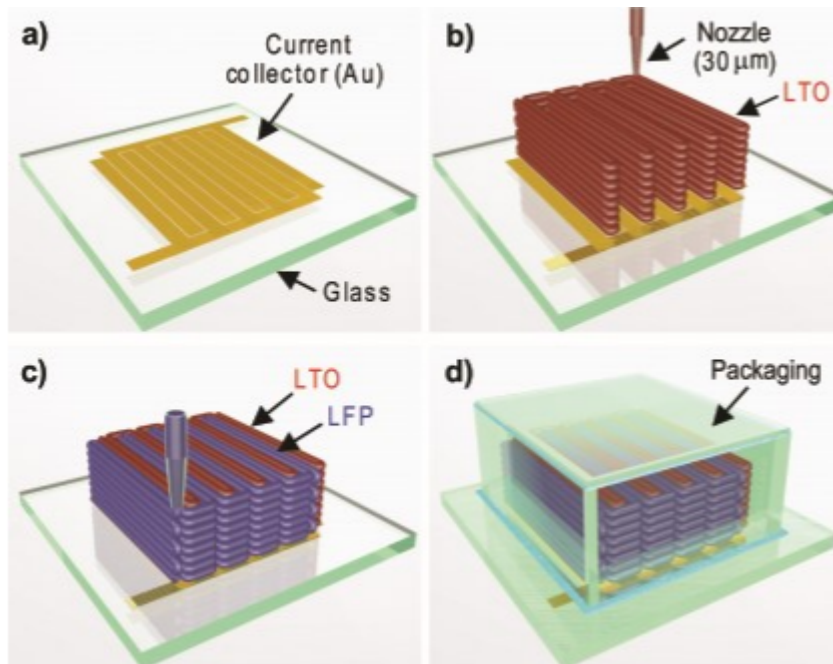


Figure 17: Optical and SEM images of the printed 16-layer interdigitated battery

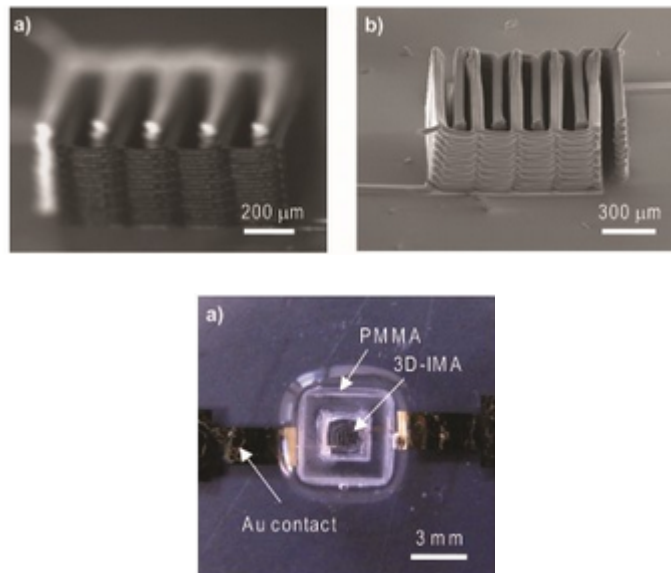


Figure 18: Fully packaged assembly

2.8.4 High Energy Density Micro-Battery Enabled by 3D Electrode and Micro-Packaging (Lai)

In 2010, researchers at MIT developed the first micro-battery less than 10 cubic millimeters that achieved energy densities that are normally created in batteries 100 times larger in volume. The cathode of the battery was made of LiCoO_2 and they used an anode of Lithium

metal. As seen in Figure 19a, a gold shell and a copper metal lid were the current collectors for the battery. The cathode is attached to the gold shell and the anode is attached to the copper lid. The researchers placed a micro-porous separator, Celgard 2325, between the two active materials. Then they electrodeposited the gold shell (100 μm thick) onto precision-machined aluminum mandrels, which they etched away using a sodium hydroxide (NaOH) solution to yield the finished shell. They then laser cut the copper lid (10 μm thick) from battery grade copper foil, punched holes into the lid and filled the holes with electrolyte. Using a light-cured adhesive the researchers bonded the lid to the shell.

The battery was able to deliver an energy density of up to 675 WhL^{-1} and a power density of 150-200 WL^{-1} for a charge voltage of 4.6V at approximately C/3 discharge rates. While maintaining good cycle life the micro-battery performed proportionally to batteries 100 times larger in size. Figure 19a illustrates the assembly of the micro-battery and Figure 19b shows the size of the battery in comparison to a US penny.

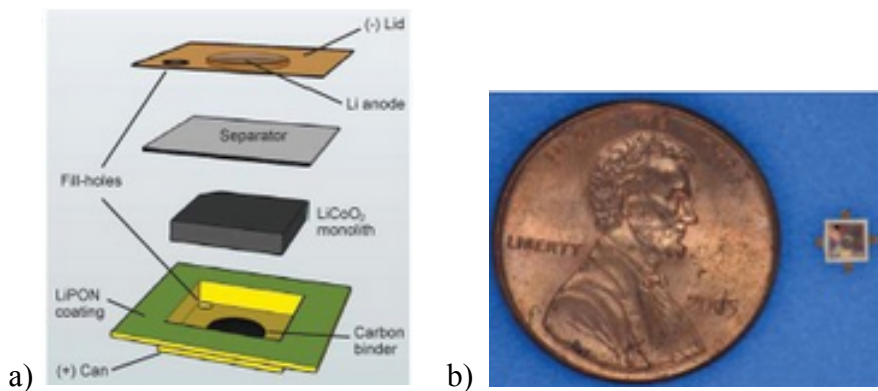


Figure 19: Thin film micro-battery

2.8.5 Our Micro-Battery: Low Cost, 3D Electrode Micro-battery

This project will involve assembling a fully functioning lithium ion micro-battery using low cost processing methods. While other micro-battery research has involved the use of complex processing and expensive materials, we will try to utilize a 3D electrode structure and

simple packaging and sealing methods to create an operational battery with competitive specific energy and capacity.

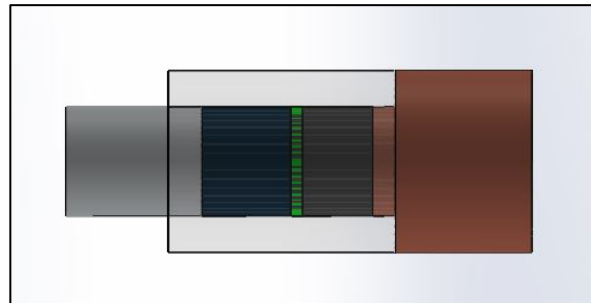


Figure 20: SolidWorks model of our proposed micro-battery

The ultimate goal of this project will be to create the smallest documented rechargeable, lithium ion battery, at a fraction of the cost and development time as the previously stated micro-battery models. The following sections will outline our novel process of making our battery and the results of our testing.

3.0 Methodology

The goal of this project was to develop a fully functioning, low cost, high energy density micro-battery. To achieve this goal, the team developed a method to assemble a battery utilizing innovative processing techniques, a three-dimensional electrode structure, an injectable polymer gel electrolyte separator, and simple, but effective packaging methods. Specifically, the team accomplished the following objectives:

1. Develop an effective packaging technique that could hermetically seal the battery
2. Develop and test a polymer gel electrolyte separator capable of being injected into the battery
3. Develop a process to build the battery that would result in successful operation
4. Perform a series of tests on the battery to measure charge capacity, energy density, and cycle life

3.1 Development and Processing of Battery Packaging and External Components

One of the greatest challenges of this project was designing an external casing for the micro-battery that would both shield the active materials from sunlight and provide a hermetic seal that would protect the battery from oxygen and water contamination, which would disrupt the internal battery chemistry.

3.1.1 Battery Housing

The team utilized glass tubes made of Pyrex glass purchased from Pegasus Glass. The glass tubes are 3mm tall with a diameter of 4mm and wall thickness of 0.8mm. Material properties for the Pyrex glass can be found in Appendix H. Glass was chosen as a battery

housing because it is low cost, has dimensional consistency, and is unreactive with the internal battery materials.

3.1.2 Selection / Preparation of Current Collectors

When considering materials for current collectors in lithium-ion battery applications there are limited options due to lithium's high reactivity with metals. High purity aluminum was chosen as the cathode end current collector and high purity copper was chosen as the anode end current collector.

3.1.3 Aluminum Current Collector

Aluminum dowel pins were purchased from McMaster Carr with a diameter of 3/32" and length of 1/2". Material properties for the aluminum dowel pins can be found in Appendix E. These dowel pins were an ideal starting material as they have very high diameter tolerances and no machining was required to fit the pin into the inner diameter of the glass tube. The tip of the pin was lightly sanded so that the pin could be interference fitted into the glass tube, creating a higher level of sealing. The interference fitting had to be performed very carefully as the Pyrex



Figure 21: Aluminum current collector being sanded

glass tubes were brittle and excessive force would shatter the tube. Additionally, an aluminum dowel pin was resistance tested using a multi-meter, and then compared to the resistance of the aluminum foil used in other batteries to determine its effectiveness for our project.

3.1.4 Copper Current Collector

Unlike the aluminum current collector, a high purity copper dowel pin could not be readily found for purchase. The team utilized 1/8" diameter Copper 145 rods purchased from McMaster Carr. The copper rod had to be precision machined to achieve a proper interference fit with the glass tube. The machining was performed in the WPI Washburn Manufacturing Labs using the CNC Lathe. Solidworks models were created of the original stock and the desired final product. The machining sequence was created in ESPIRIT, where tool paths, tool types, and feed rates were specified.



Figure 22: Aluminum dowel pin current collector after sanding to insure interference fit (Left) Copper current collector after machining and sanding (Right)

Additionally, a copper rod was resistance tested using a multi-meter, and then compared to the resistance of the copper foil used in other batteries to determine its effectiveness for our project.

3.1.5 Machining Copper Rod

The team was concerned that significant deflection could occur during machining since copper is an inherently soft material. To minimize deflection, just ¼” of the rod was allowed to protrude from the lathe lock. After several trials, it was concluded that adequate machining consistency was achieved. The copper rod was machined down to 0.0944”; slightly larger than the inner diameter of the glass tube, so that an abrasive process of light sanding could be performed to create an interference fit with the glass tube.

3.1.6 Adhesive Sealant

The current collectors were sealed to the glass tube using Loctite 2 part Quick Set Epoxy. The Loctite 2 part Quick Set Epoxy was ideal for our application because it was rated for glass to metal adhesion, was low cost, set in 5 minutes, fully cured in 24 hours, was rated for up to 150 °C, was water resistant, and could cure in the absence of oxygen, such as in a glove box atmosphere.

3.1.7 Hermeticity Testing of Battery Packaging

To develop a successful battery, it was important to ensure that the cell was properly sealed. To that end, our team developed a method to test the sealing ability of our battery housing. To carry out this test, a small sample of lithium metal was sealed in a battery housing using the same assembly and sealing procedures as were used for the other battery prototypes.



Figure 23: Lithium metal sealed inside battery prior to hermiticity test

We then submerged the sealed sample in 3 inches of water and allowed the sample to remain undisturbed in a vial for two weeks. We used lithium metal in this test because lithium is highly reactive with water and if a leak were present the lithium would disappear due to the reaction.

3.2 Development and Processing of Internal Battery Components

Because of the small scale we were working on, novel techniques had to be used in order to process the internal materials of our battery. This included developing a polymer gel electrolyte separator, creating slurries of the anode and cathode materials, and being able to control the amounts of material that were used in each battery.

3.2.1 Polymer Gel Electrolyte Separator

In this project, a 1:1 homogenous blend of PVDF and PMMA was developed, due to its ease of processing. Although this structure of PGE was studied as part of the research done by H.P Zhang et al as discussed in section 2.6.2, we performed further testing in order to determine its cycling ability and effectiveness as a separator. The PGE was created by combining an equal mass of PVDF powder and crystallized PMMA in a vial with N-Methyl-2-Pyrrolidone (NMP)

solvent, and then mixing the solution for 24 hours on a magnetic stir plate. After a homogenous mixture was achieved, a thin film of the solution was deposited on a glass slide and allowed to dry in a 60°C oven (or on a 60 °C hot plate) for 12 hours. Next, a sample of the film was taken from the glass slide and was soaked in liquid electrolyte for 24 hours, allowing for complete saturation of the PGE.

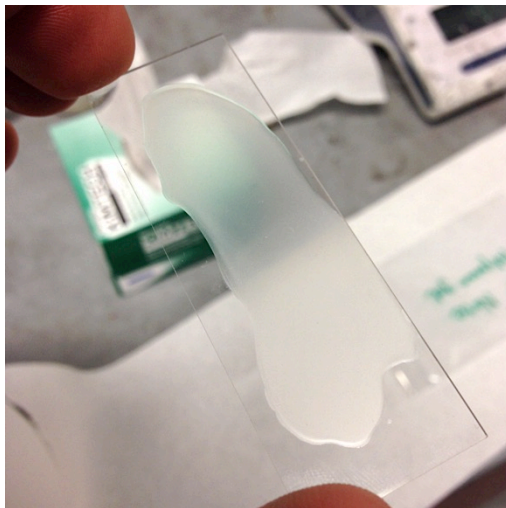


Figure 24: Homogeneous PMMA/PVDF PGE film prior to electrolyte saturation

Testing of the PGE was conducted using a Teflon Swagelok cell, utilizing a lithium metal anode and a LiCoO_2 cathode on an aluminum foil current collector. The cell was filled with liquid electrolyte and sealed inside an Argon glove box. The cell was then tested using an ARBIN electrochemical testing system, which allowed for the control of charge and discharge current, as well as minimum and maximum charging potentials. Using this system, charge - discharge capacity could be measured, as well as cycle life, charge - discharge energy, and charge - discharge duration.

3.2.1 Anode

Several materials are compatible for use as the anode, but for this project a graphite anode was selected due to its chemical stability and ease of handling. The anode was produced

by first creating a slurry of conductive graphite, C65 carbon, and a 2.5% binder solution composed of 1-Methyl-2-pyrrolidone (NMP), an organic solvent, and Polyvinylidene Fluoride (PVDF).



Figure 25: Electrode components from left to right: Conductive Graphite, LiCoO₂ Powder, C65 Carbon, 2.5% Binder Solution of PVDF in NMP

These three components were combined in the mass ratio of 80% conductive graphite, 10% C65 carbon, and 10% binder. The 10% binder refers to the mass of binder after the solvent has been evaporated. When the binder was a solution, this ratio changed to ~0.16% conductive graphite, ~0.02% C65 carbon, and ~81.63% binder solution. These components were combined using a mortar and pestle, mixing for 2 to 3 minutes.

3.2.2 Cathode

For this project, lithium cobalt oxide (LiCoO₂) was used for the cathode material due to its high specific energy compared to other common cathode materials, as well as its availability in the laboratory inventory. The cathode was produced using a similar method as the anode, replacing conductive graphite with LiCoO₂ powder. Additionally, the same ratio of materials was used, with 80% LiCoO₂, 10% C65 carbon, and 10% of the same binder solution. The

components were combined using a separate mortar and pestle from the anode to avoid contamination, and were mixed for 2 to 3 minutes.

3.2.4 Measuring the Mass per Droplet of the Active Materials

As we used very smaller amounts of active material in our battery, it was vital that we could accurately control and predict the amount of material being added. For both the anode and the cathode, a micropipette was used to deposit the material slurry on to the current collectors.

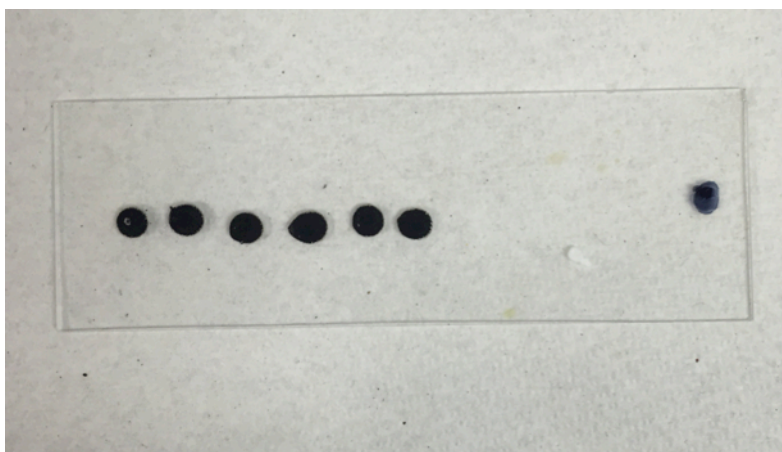


Figure 26: 6 Drops of electrode were deposited on a glass slide and then allowed to dry. The total mass of electrode material was measured, then divided by 6 to estimate the mass of each droplet of electrode.

To measure the mass per drop of our active materials, we initially obtained a glass slide and measured its weight. We carefully applied six drops of active material slurry to the slide and re-weighed the sample. We then dried the sample in a 60 °C oven and re-weighed the dried sample. We calculated the weight of one drop of active material by subtracting the weight of the glass slide from that of the dried sample, and divided that result by six. We carried out this process to determine the weight per droplet of both the anode and cathode.

3.3 Assembly and Packaging of Battery Unit

Designing a process to construct the battery was and continues to be the most difficult part of this project. Reported here are our current methods used to assemble the batteries, although these methods are still in development.

3.3.1 Initial Half Assembled Cell

The battery assembly began by first creating a half assembled cell. This entailed sealing one end of the glass tube with a current collector. The half-cell could be built with either the aluminum or copper current collector depending on which internal battery component was to be injected first.

3.3.2 Assembling the Half Cell

1. Take aluminum dowel pin and abrasively reduce a section of about 3/32" from one end until the metal fits tightly into the glass tube creating an interference fit. It was crucial that the sanding process was performed uniformly around the rod or pin.



Figure 27: Aluminum dowel pin current collector prior to sealing. Dowel pin and glass cylinder form a interference fit.

2. Using a paper towel, any excess metal was wiped from the tip of the metal.
3. The 2-part quick set epoxy was then dispensed onto an aluminum foil sheet or any other disposable surface and mixed for 1 minute.

4. The tip of a fine point nail was coated with the epoxy and applied to the corner between the glass and the metal.
5. The half assembled cell was rotated for ~5 minutes to insure the epoxy would not drip off during the setting period.
6. The half assembled cell was then left to dry for 24 hours.

3.3.3 Assembly of Internal Battery Materials

Once the adhesive on the half assembled cell was fully cured, the half-cell was placed in an alligator clip assembly rig for further processing. The assembly rig consisted of 4 alligator clips on a heat resistant base, allowing for simultaneous processing of multiple batteries.

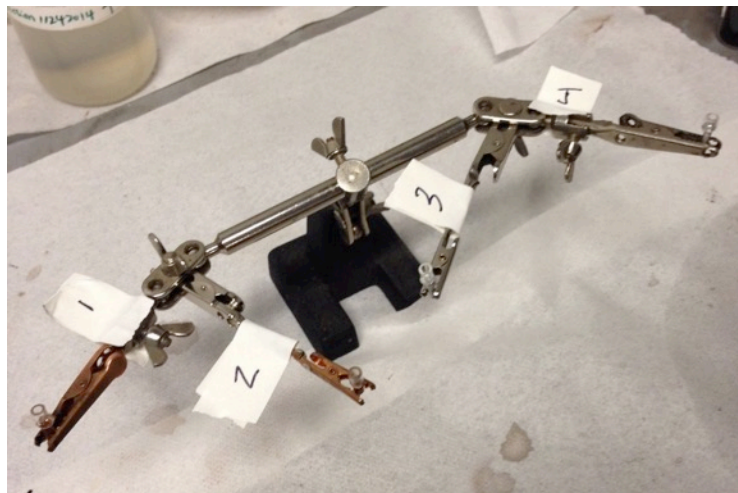


Figure 28: Alligator clip assembly rig for micro-batteries

Cathode

As the half assembled cell was typically built on the aluminum current collector, the cathode was the first electrode to be added to the cell. A slurry of the cathode materials was prepared according to the method described above, and then a glass micro-pipette was used to insert the slurry into the cell. The high viscosity of the slurry made this process very difficult. In order to take material into the pipette, only a very slight squeeze of the pipette bulb was possible,

otherwise sputtering of the slurry inside the pipette would occur and it would be impossible to inject the material. The cell was completely filled with the cathode material, and then allowed to dry in a 60 °C oven for 24 hours. The dried cell was then removed, and the cathode material was compressed by applying finger strength pressure for 15 seconds to an aluminum peg, which was sized to exactly fit into the glass housing. Figure 29 shows the end product of the cathode injection process.

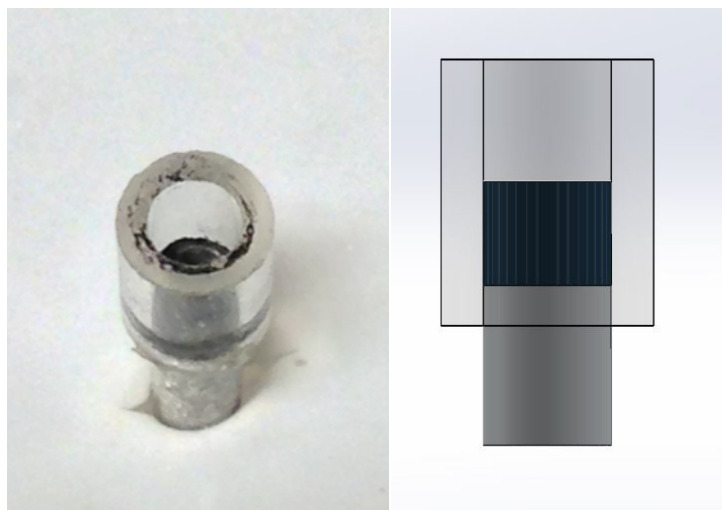


Figure 29: Final product of cathode injection into the battery housing. Actual process (Left) Schematic of the process (Right)

Physical Gap Separator Method

In this method, instead of using a PGE separator between the electrodes, a physical space was left between the anode and cathode to act as the separator. This method insured that no shorting will occur in the battery, but caused difficulty maintaining a minimal distance between the electrodes as is possible with a PGE separator. Figure 30 below shows the fully assembled “gap separator” battery, back lit with an LED light to clearly show the space between the electrodes. The orange tint in the gap is caused by the degradation of the liquid electrolyte.



Figure 30: LED backlit image of gap separator battery

This alternate method of building the battery was used as an intermediary step to building the complete battery featuring a PGE separator. This “gap battery” allowed us to test the effectiveness of all other battery components before adding in the PGE, as the PGE led to unique challenges when implemented in the battery.

Polymer Gel Electrolyte Separator Method

It was our ultimate goal of this project to assemble a battery utilizing a physical, PGE separator in order to minimize the separation between the electrodes, while preventing short-circuiting and maintaining efficient ion transport. For this method, a polymer gel electrolyte separator was developed according to the method described above. When the PGE was implemented into the battery, it was injected directly into the glass battery casing and allowed to dry on top of the cathode. In this way, a separator was produced that matched the width of the battery casing, and could completely separate the anode and cathode. Once dry inside the casing, the battery was moved into the argon glove box, where liquid electrolyte was injected into the battery, allowing the PGE to become saturated and form a gel. Figure 31 below shows the battery with the PGE solution injected on top of the cathode, before drying has occurred.

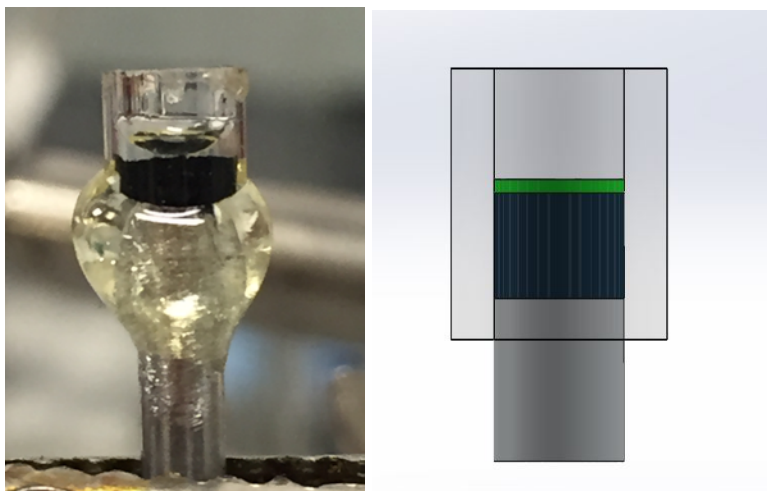


Figure 31: PGE injected into battery to dry on top of cathode and form to battery casing. After drying, PGE will be saturated with liquid electrolyte to form gel. Actual process (Left) Schematic of process (Right)

Anode

A slurry of the anode materials was prepared according to the method described above. To ensure proper adhesion to the current collector, the anode slurry was deposited directly onto copper current collector using a micropipette, and was allowed to dry in a 60 °C oven for 24 hours. We found that this method created a much better connection between the anode and current collector, than our previous stacking method, explained in Appendix I.



Figure 32: Post processing images of anode deposition onto copper current collect. Actual process (Left) Schematic of process (Right)

3.3.4 Final Processing

Once the cathode and separator (Or just the cathode in the gap separator method) were dried and assembled into the cell, the cell was filled with liquid electrolyte and final assembly and sealing of the battery took place inside the argon glove box. This step had to happen in the glove box because the liquid electrolyte was extremely sensitive to oxygen and water.

Injection of the Liquid Electrolyte

Before the battery was sealed with epoxy, the remaining cavity was filled with liquid electrolyte in order to insure that maximum saturation of the electrodes and the PGE separator occurred. The liquid electrolyte was injected into the battery use a micropipette.

3.3.5 Final Sealing

Once the electrolyte was properly injected into the cell, the anode (built onto its corresponding current collector) was inserted into the cell in the same manner as described in assembling the original half-cell. It was important to apply proper force to the current collector in order to press the components together to assure maximum surface contact, but to avoid breaking the cell or damaging the internal components, which could potentially cause a short-circuit. The epoxy adhesive was applied in the same fashion as described in assembling the half-cell, but the level of processing difficulty was greatly heightened due to the constraints of the glove box. Once the adhesive had set, the cell was put under a light shielding cover due to the liquid electrolytes sensitivity to UV light. The adhesive was then left to fully cure for 24 hours.

3.3.6 Light Shielding

Once the epoxy sealing had fully cured, the complete battery was removed from the glove box. To insure the stability of the electrolyte during testing, which would occur in a well-lit, standard atmospheric environment, a strip of black electrical tape was wrapped around the

battery to block light from reaching the battery. This method allowed us to keep the batteries in the lab environment during testing, without significant harm to the battery internal components.

The fully assembled batteries can be seen in the figures below.



Figure 33: Top Left: Fully assembled PGE separator battery. Top Right: Fully assembled gap separator battery. Bottom: Micro-battery with electrical tape wrapping for light shielding

3.4 Battery Testing

As mentioned above, an ARBIN electrochemical testing system was used to perform all testing of the batteries. This system consisted of a large module, which could support multiple testing channels, and worked in conjunction with computer software to control testing parameters. The testing system setup can be seen below in Figure 34. In order to determine the performance of the battery, the two most important functions of the battery to be tested were the battery's charge capacity and cycle life.



Figure 34: The ARBIN electrochemical testing system with testing module and computer shown

To determine charge capacity, a series of tests were planned using a systematic increase in charging and discharge current. These tests were a function of the battery's theoretic charge capacity or "C" which was determined from the follow equation based on the mass of LiCoO_2 present in the cathode:

$$\frac{\left[\text{mass}_{\text{cathode}}(g) * 0.8 * 137 \frac{\text{mAh}}{g} \right]}{1000 \text{ mA/A}} = C \text{ (Amps)}$$

The "0.8" value in the equation refers to the weight percent of LiCoO_2 present in the cathode, with the other 20% of mass being made up by C65 carbon and PVDF binder. The value of "C" was then divided by the theoretical charging time in hours, to give an approximate rate at which the battery would charge. To test the effectiveness of the battery, one complete charge – discharge cycle was to be completed at C/10 (One tenth of the theoretical charge capacity), C/5, C/3, C/2, C, 2C, 3C, and 5C, where these values affected the rate at which the battery charged. During these tests, the consistency of the charge and discharge capacity was to be monitored. Next, the battery was to be cycle tested at "2C", and allowed to charge and discharge as many

times as possible before the battery failed. In this test, we were hoping to see the battery cycle at least 50 times before failure.

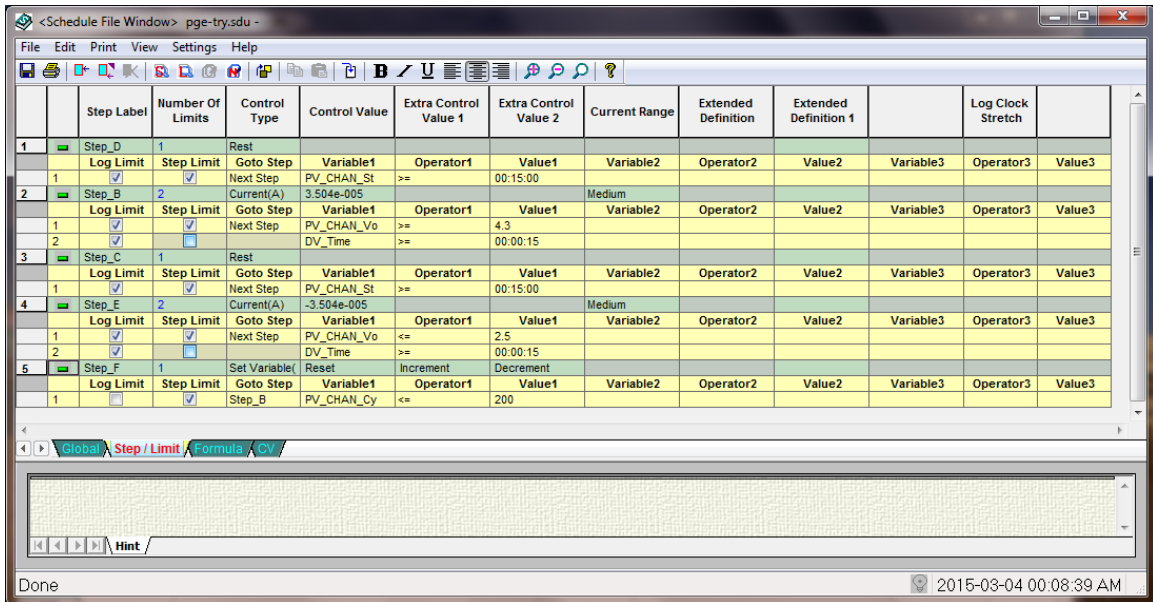


Figure 35: Screen shot of the charging test design screen from the ARBIN software

Using the ARBIN software, we designed a testing program to control the charge and discharge rates of the batteries. Additionally, minimum and maximum potentials were set at 2.5 volts and 4.3 volts respectively to avoid over charging, and to keep the battery in its optimal range. The test was designed to take data from the battery ever 15 seconds, in order to produce accurate charging and discharging curves. While the charging / discharging current changed for each test, a typical testing procedure was as follows:

- 1) Battery rests for 15 minutes after being connected to electrochemical tester
- 2) Battery is set to charge at specified current until it reached 4.3 V
- 3) Once at 4.3 V, the battery rests for another 15 minutes to test its ability to hold potential
- 4) Battery is set to discharge at specified current (opposite of charging current) until it reached 2.5 V
- 5) This cycle was set to repeat 200 times, or until the battery failed or the test was stopped

4.0 Results & Discussion

In this section we will present the results of all testing that was done on both the individual components of the batteries and on the batteries themselves. We will first go through our findings on the strength of the battery's glass housing as well as its ability to create a hermetic seal around the internal battery components. Next we will discuss the results of the PGE testing, and what these results mean for the overall performance of the battery. Finally, we will present the testing results of each battery that we assembled, what we learned from each successive test, and discuss how our battery evolved throughout the course of this project in order to get closer to our goal of a fully operational battery.

4.1 Determining the Allowable Internal Stress of the Glass Battery Housing

In order to prevent the glass battery housing from cracking or breaking during the assembly process, it was essential for us to know the maximum internal stress that the glass could withstand. This information was also vital when considering the strength requirements of the potential applications of our micro-battery. The internal stress has three components: the stress in the axial direction, the stress in the radial direction and the stress in the longitudinal direction. To complete this analysis, we calculated the hoop stress, σ_t , the radial stress, σ_r and the longitudinal stress, σ_l given the following dimensions:

- Internal radius, $R_i = 1.2\text{mm}$
- Outer radius, $R_o = 2\text{mm}$
- Wall thickness, $t = 0.8\text{mm}$

The glass tube was considered to be a thick walled cylinder because the $\frac{R_i}{t}$ characteristic was < 10 , and in this case, the hoop and radial stress occur in the wall of the tubes. The hoop stress acts

in the axial direction and the radial stress acts in the radial direction. Figure 36 below presents a schematic of the analysis.

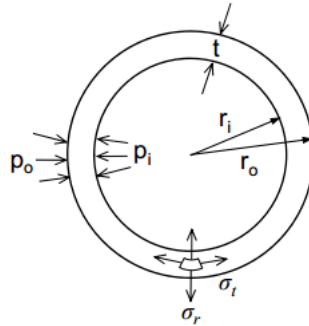


Figure 36: Schematic of internal stress analysis

We calculated both the hoop and radial stress over a range of values for internal pressure and plotted the results on separate graphs. To determine the maximum internal stress, we set both the hoop and radial stress equal to the tensile strength, T , of the glass. After setting these values as the tensile strength, we simply read the corresponding values of the internal stress from the graphs. We used the following parameters in the analysis:

$T_s := 6.89 \cdot 10^6 P_\varepsilon$	Tensile strength (<i>see appendix ##</i>)
$R_i := 1.2 \text{mn}$	Inner radius
$R_o := 2 \text{mn}$	Outer radius
$P_o := 1 \cdot 10^5 P_\varepsilon$	External pressure (<i>atmospheric pressure</i>)
P_i	Internal pressure (calculated parameter)

4.1.1 Calculating the Hoop Stress, σ_t

We set the hoop stress equal to the tensile strength by plotting the function, $\sigma_t(P_i)$, and T on the y-axis and found the point where both lines intersect. From there, we read the corresponding value of internal stress. Using the trace function in MathCad, we found that the

maximum allowable internal stress in the axial direction was found to be approximately 3.43MPa.

$$\sigma_t(P_i) := \frac{P_i \cdot R_i^2 - P_o \cdot R_o^2 - R_i^2 \cdot R_o^2 \frac{(P_o - P_i)}{R_i^2}}{R_o^2 - R_i^2}$$

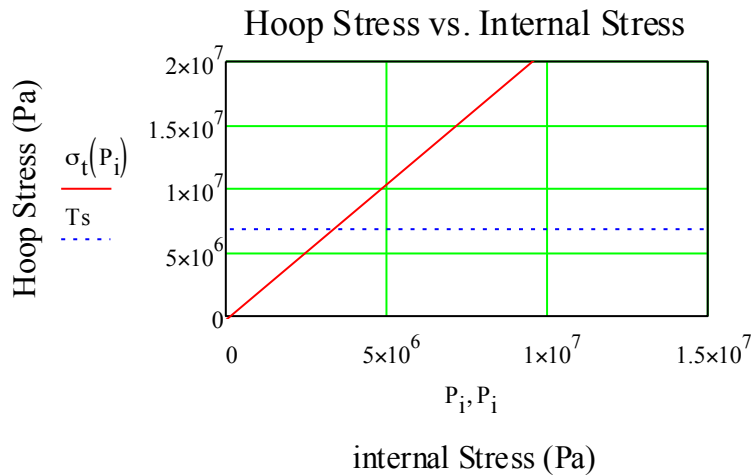


Figure 37: Graph of hoop stress vs internal pressure

4.1.2 Calculating the Radial Stress, σ_r

The graph has a negative slope because the internal stress is larger than the external stress. Based on Figure 36, we assumed that P_o acted in the positive direction therefore, P_i is in the negative direction. Using the trace tool again, the maximum internal stress acting in the radial direction was found to be approximately -6.81MPa.

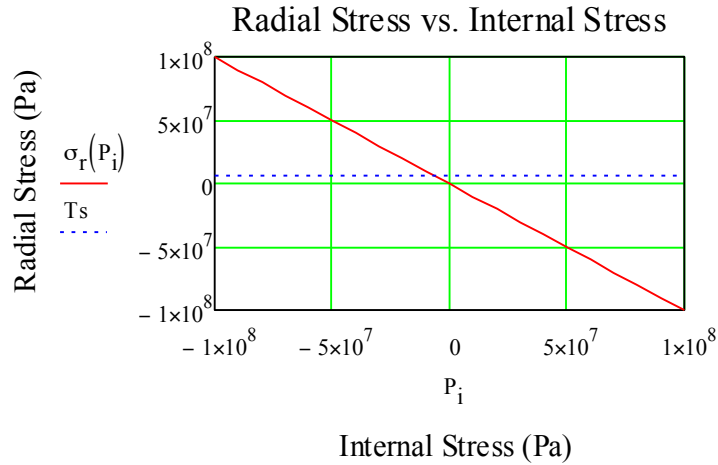


Figure 38: Graph of radial stress vs internal stress

4.1.3 Calculating the Longitudinal Stress, σ_l

Once we sealed the battery, we determined the maximum allowable internal stress in the longitudinal direction. To complete this analysis, we used the same procedure that we used to determine the maximum allowable stresses in the other directions.

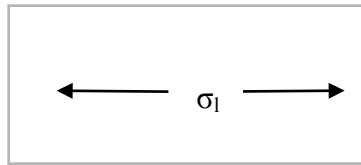


Figure 39: Longitudinal Stress

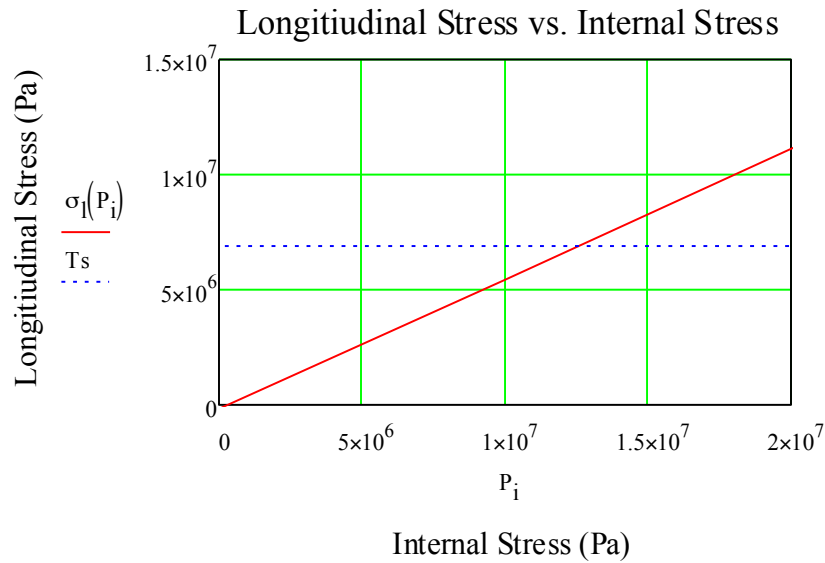


Figure 40: Graph of longitudinal stress vs internal stress

Using the trace tool once again, the maximum allowable internal stress in the longitudinal direction was found to be approximately 12.7MPa.

4.2 Hermiticity and Component Testing

Several tests were conducted on the individual components of the battery to confirm their effectiveness. These tests included a hermiticity testing of the battery housing, a mass approximation test to determine the mass of each droplet of electrode material, and a resistance test to determine the effectiveness of our current collector materials.

4.2.1 Hermiticity

On completing the hermiticity test, the team observed that none of the lithium metal had reacted with the water after two weeks of submersion and the sample was still present in the sealed battery housing. Based on these results, we conclude that the sealing process was hermetic to water.

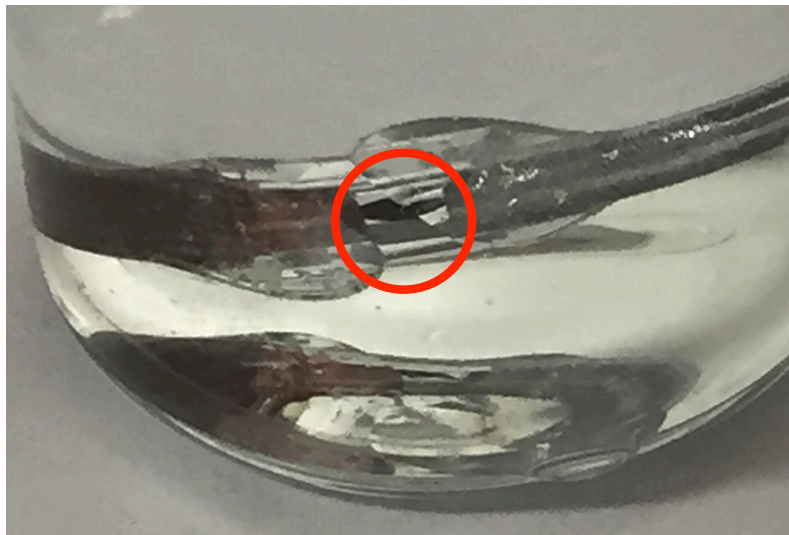


Figure 41: The sample of lithium metal is still present after 2 weeks of being submerged in 3 inches of water

4.2.2 Electrode Droplet Mass Testing

While this was a very simple test, it was very important when trying to match the amounts of anode and cathode. The average mass of one drop of cathode was found to be 0.00107 grams. The average mass of one drop of anode was found to be 0.00065 grams. The following table shows the complete results of these tests.

Table 3: Summary of Droplet Mass Approximation Test

Anode	Mass (g)	Cathode	Mass (g)
Glass Slide Mass	4.7787	Glass Slide Mass	4.7787
6 Drops Anode Wet	4.7981	6 Drops Cathode Wet	4.8091
6 Drops Anode Dry	4.7826	6 Drops Cathode Dry	4.7851
Avg Mass Anode per Drop	0.00065	Avg Mass Cathode per Drop	0.00107

4.2.3 Current Collector Resistance

Both the aluminum and copper foils used in known successful battery tests had resistance readings of 0.1 ohms. Additionally, both of our current collector materials, the aluminum dowel pins and the copper rods also had resistance readings of 0.1 ohms.



Figure 42: Resistance testing of current collector materials

These results showed that our chosen current collector materials would not cause any additional resistance to electron flow, and were acceptable to use in our batteries.

4.3 Polymer Gel Electrolyte Testing Results

To ensure that the PGE separator we utilized worked properly, we performed charge – discharge testing using a Swagelok cell. Below in Figures 43 - 45 are the charging test results for the separator using a lithium metal anode and LiCoO₂ cathode in the Swagelok cell at various charging rates. Based on the theoretical capacity of the cell, the charging currents utilized were C/10, C/5, and C/1.

$$\text{Mass of Cathode} = 0.0011 \text{ g}$$

$$C = \frac{\left(m_{\text{Cathode}} * 0.8 * 137 \frac{\text{mAh}}{\text{g}}\right)}{1000 \frac{\text{mA}}{\text{A}}} = \text{Ah}$$

$$C = \frac{\left[(0.0011 \text{ g}) * (0.8) * \left(137 \frac{\text{mAh}}{\text{g}}\right)\right]}{1000 \frac{\text{mA}}{\text{A}}} = 0.00012056 \text{ Ah}$$

Therefore, the charging currents were as follows:

$$\frac{C}{10} = 1.2056 \times 10^{-5} \text{ Amps} \quad \frac{C}{5} = 2.4112 \times 10^{-5} \text{ Amps} \quad \frac{C}{1} = 1.2056 \times 10^{-4} \text{ Amps}$$

The purple line in the graphs below indicates the voltage of the cell and the blue line indicates the capacity of the cell. The results came out as expected with typical battery charging curves for the corresponding electrodes. The results show a charge – discharge capacity of approximately 80% - 90% (0.0964 mAh - 0.1085 mAh) of the theoretical capacity (0.1206 mAh).

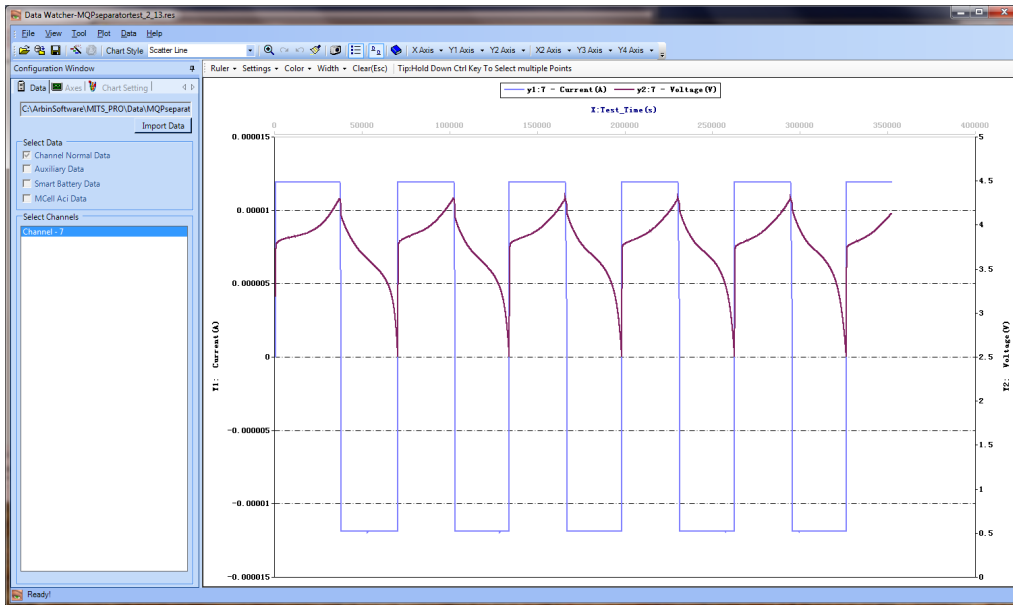


Figure 43: Charging curve test results for PGE separator in Swagelok cell at C/10 charge rate

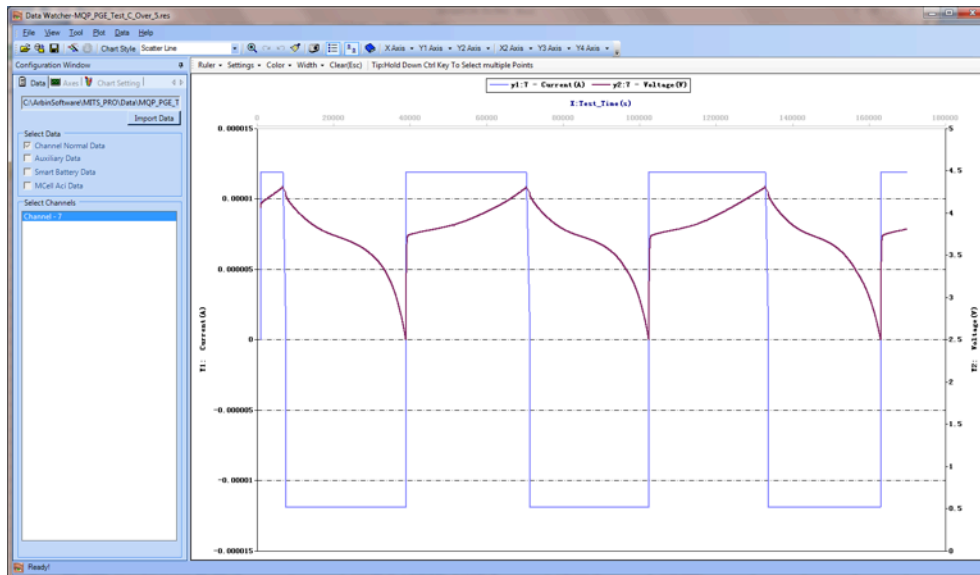


Figure 44: Charging curve test results for PGE separator in Swagelok cell at C/5 charge rate

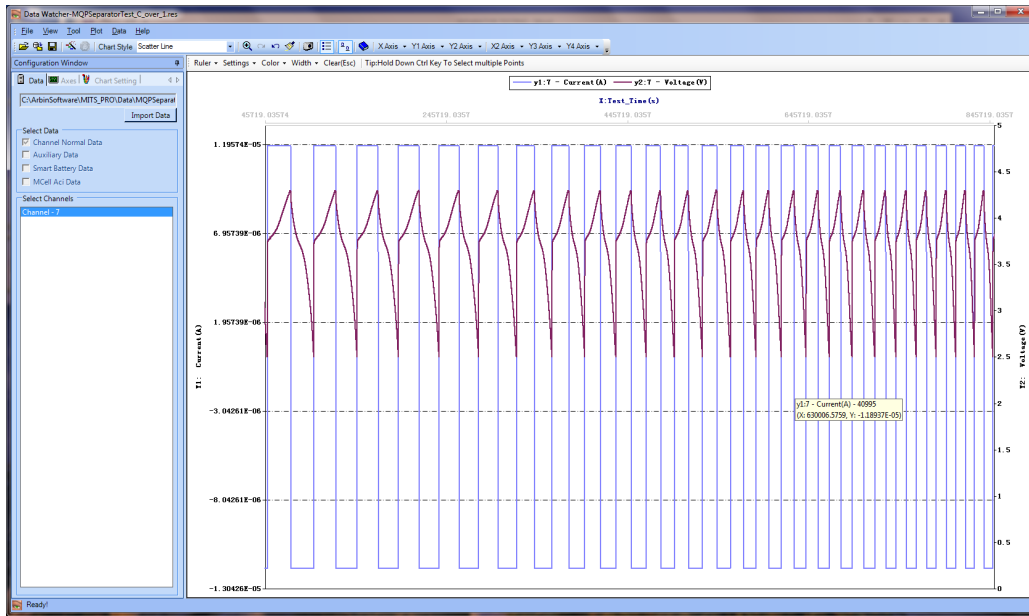


Figure 45: Charging curve test results for PGE separator in Swagelok cell at C/1 charge rate

Figure 46 illustrates the significant decrease in capacity retention after 30 plus cycles. These are expected results for a lithium anode battery since volume expansions and contractions during charging and discharging cause significant cracking and internal flaws in the anode, which eventually lead to cell failure.

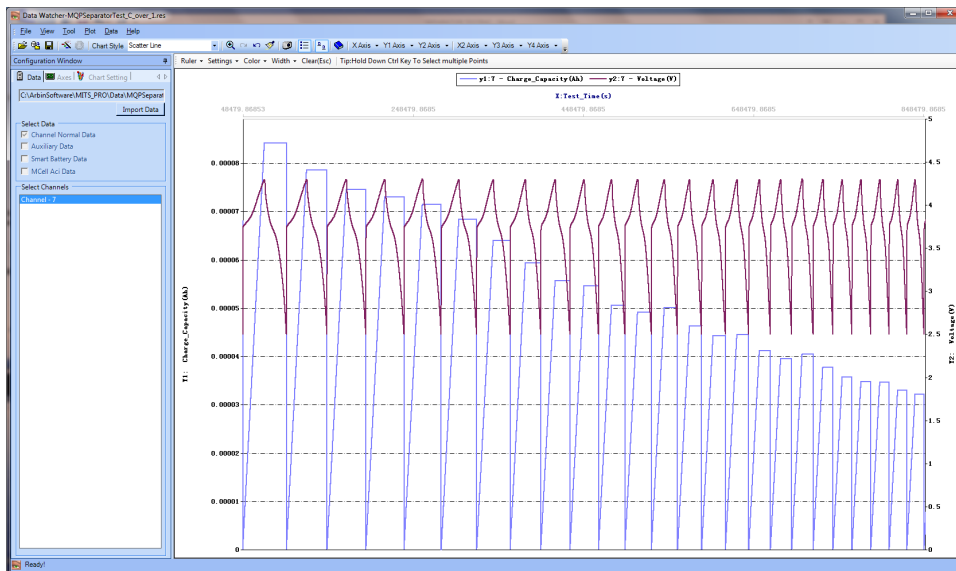


Figure 46: Charging capacity test results for PGE separator in Swagelok cell at C/1 charging rate, capacity is greatly diminished after 30 cycles

4.4 Battery Capacity Testing

Several methods were attempted to make the micro-battery. Here, we will discuss the calculated theoretical capacity and energy density of our battery, as well as the results of the testing of each of these methods. These test results helped us determine what was happening inside the battery and how we could make each successive battery better.

4.4.1 Theoretical Calculations

Givens:

- *Specific Capacity of LiCoO₂ Cathode: 0.137 Ah/g*
- *Specific Capacity of Graphite Anode: 0.372 Ah/g*
- *Voltage Potential between Cathode and Anode: 3.8 V*
- *Average mass of battery cathode = 0.0015 g*
- *Average mass of battery anode = 0.0027 g*
- *Average mass of battery = 0.904 g*

Notes:

- *Since specific capacity of anode is 2.7 times greater than the cathode then to match electrode performance the mass of the cathode should be 2.7 times greater than the anode.*

- *In this situation the cathode was not optimized and is the limiting factor. Thus, all battery calculations were based on the cathode.*

- *The active materials within the cathode, which is the LiCoO₂ accounts for 80% of the overall mass*

Since the limiting electrode was the LiCoO₂ cathode, the first step was to calculate the theoretical energy density of this cathode using the potential between LiCoO₂ and Graphite:

$$\text{Theoretical Specific Energy of Cathode} = \frac{W * h}{g} = \frac{V * Ah}{g} = \frac{3.8 * 0.137}{g} = 0.5206 \frac{Wh}{g}$$

The total theoretical energy of the battery could be calculated by multiplying the theoretical energy density of the LiCoO₂ by the total mass of cathode within the battery:

$$\textit{Theoretical Energy of Battery} = 0.5206 \frac{\textit{Wh}}{\textit{g}} * 0.0015 \textit{ g} * 0.8 = 0.0006247 \textit{ Wh}$$

By dividing the total theoretical energy of the battery by the total mass of the battery, the theoretical energy density of the battery could be calculated:

$$\textit{Theoretical Specific Energy of Battery} = \frac{0.0006247 \textit{ Wh}}{0.904 \textit{ g}} = 0.000691 \frac{\textit{Wh}}{\textit{g}}$$

A common performance metric of batteries is their capacity. By multiplying the specific capacity of \textit{LiCoO}_2 by the total mass of the cathode within the battery the battery capacity can be calculated:

$$\begin{aligned} \textit{Theoretical Capacity of Cathode} &= 0.137 \frac{\textit{Ah}}{\textit{g}} * 0.0015 \textit{ g} * 0.8 = 0.0001644 \textit{ Ah} \\ &= 0.1644 \textit{ mAh} \end{aligned}$$

4.4.2 First Battery Using Stacking Method

A common issue that the team ran into during the initial prototyping stages was short-circuiting of the battery. This was caused when the anode and cathode came in contact, which caused the battery to fail because the cell could not build adequate potential between the electrodes. Below, Figure 47 and Figure 48 are two data sets for short-circuited batteries. In Figure 47, the voltage stays very low because as electrons begin to concentrate in the anode during charging, they are able to freely flow across the battery and no driving force is created for lithium ions to move from the cathode and intercalate in the anode. This was a sign that the short-circuiting in the battery was severe.

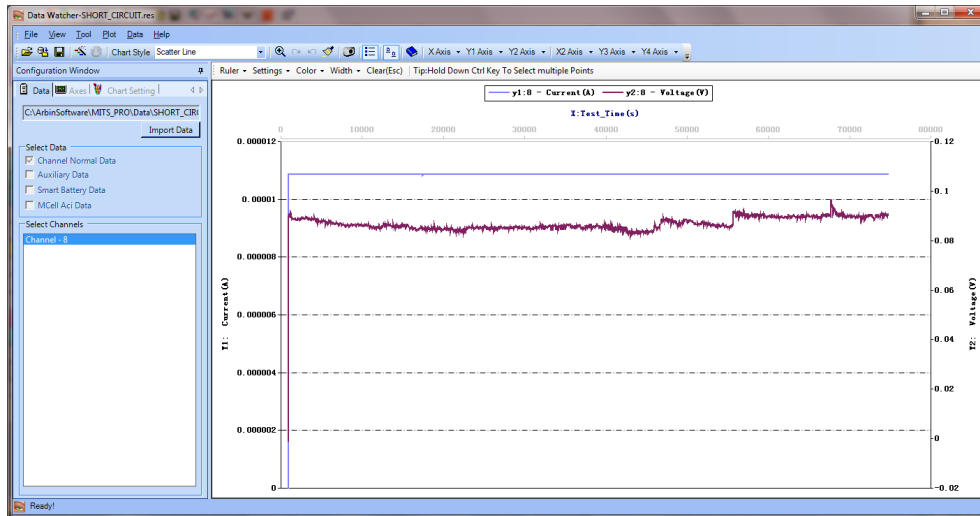


Figure 47: Charging curve test results for an extensively short-circuited battery

In Figure 48 the voltage fluctuates in a volatile manner. This would indicate a slight short-circuit, meaning the contact between the cathode and anode may be very miniscule. The fluctuating results seen in Figure 48 could also be caused by factors such as: poor electrode to current collector adhesion, poor electrolyte distribution, or contaminating reactants within the cell. Mainly, these graphs illustrate the sensitivity of our batteries to short-circuiting. To combat such issues the team doubled the separator size to ensure the cathode or anode would not protrude through the separator to the other electrode, and utilized a direct electrode to current collector dripping method to improve adhesion.

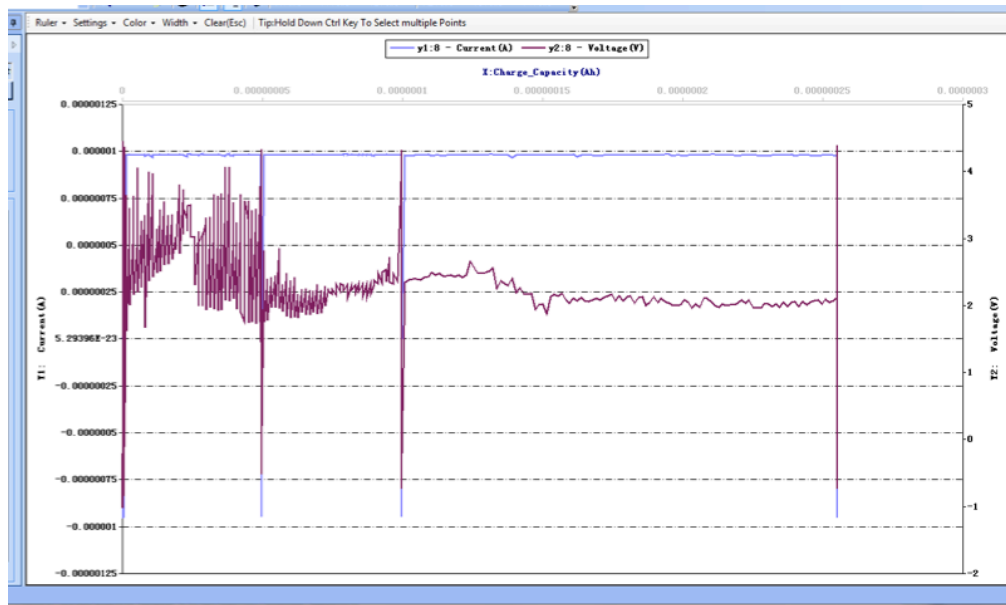


Figure 48: Charging curve test results for a slightly short-circuited battery with other failure mechanisms possible

4.4.3 Dripped Anode No Separator Method

To combat short-circuiting and other potential separator issues, the team first implemented a gap separation method where the electrodes were inserted into the cell in such a way that there was no contact. The electrodes were directly dripped and sintered onto their respective current collectors instead of solution stacking as in the previous batteries. The testing results from this battery proved to be the most promising of our tests. Figure 49 shows the charge – discharge curve from the most successful gap separator battery we assembled. The first cycle of this test matches the desired charge - discharge curve seen in standard batteries.

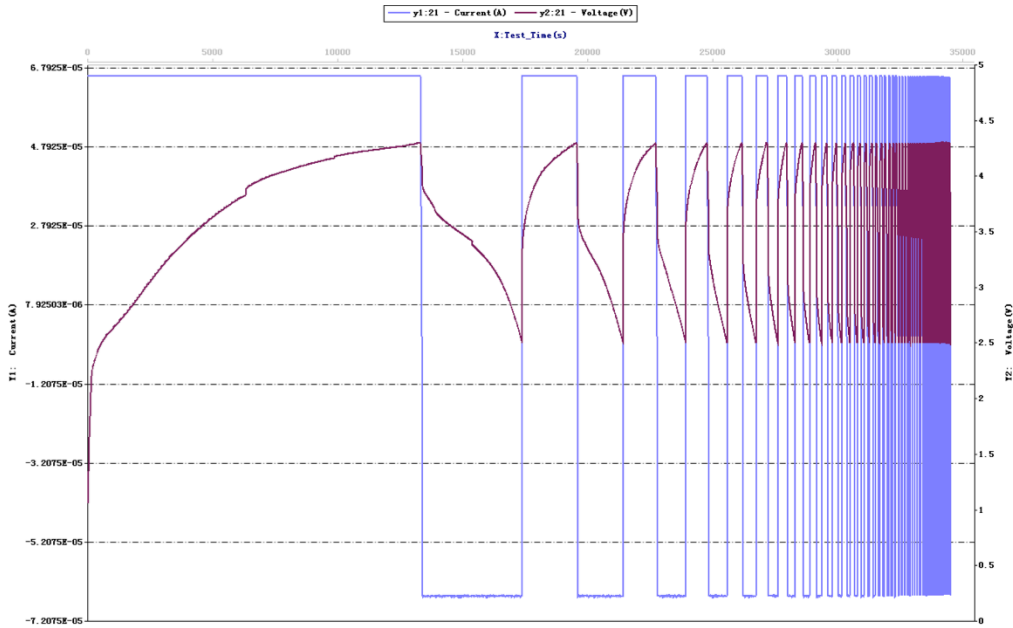


Figure 49: Voltage and Current vs Time for the gap separator battery

For this test, the resting step in the battery test plan (as described in section 3.4) was reduced from 15 minutes to 1 minute. This was done due to the realization that our batteries were having difficulty maintaining potential after charging. Reducing the rest time allowed us to discharge the battery in a controlled manner before the battery lost its potential due to other causes. This loss of potential could be related to imperfections in adhesion of the electrodes to the current collectors or from poor electrode structure, which could have prevented proper intercalation of lithium ions into the anode during charging. The charge capacity can be seen in Figure 50, represented by the blue line. The cell produced a maximum charge capacity of ~ 0.243 mAh; which was approximately 35% of its theoretical maximum. While this value was quite low, it still signified a working cell that was able to charge, despite not being optimized.

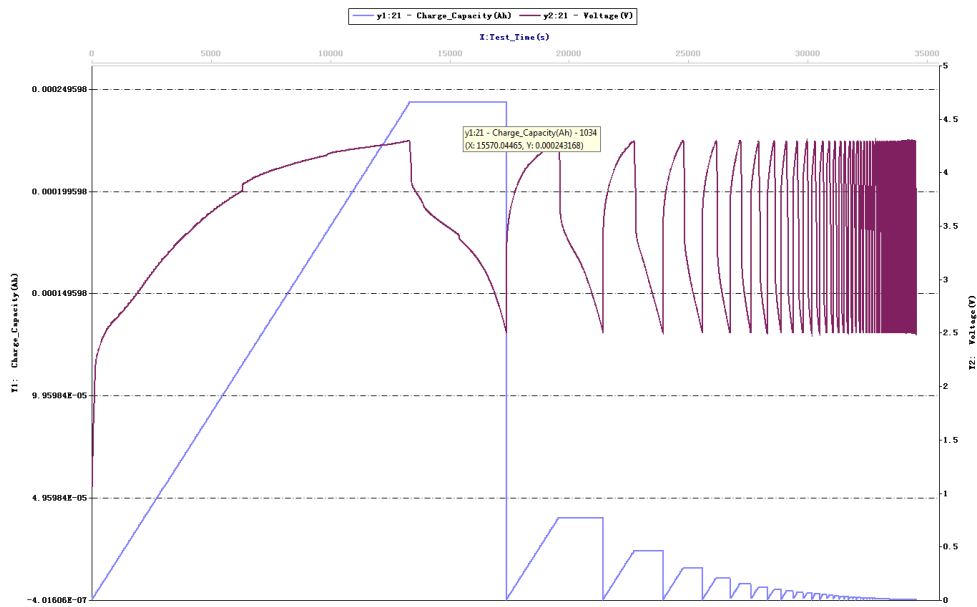


Figure 50: Charge capacity (Blue) for the gap separator battery

Figure 51 illustrates the discharge capacity, which was quite small (~ 0.0694 mAh, 10% of theoretical maximum). This meant that the cell could not sufficiently release the held charge capacity back through the current collectors. This was a common theme throughout all of our battery testing. As mentioned before, it was observed that our batteries had difficulty maintaining potential once being charged, and this flaw was most likely the cause of the very small discharge capacity observed. Additionally, this inability to maintain potential was likely the cause of the very short cycle life (2 to 3 cycles max) that we observed during these tests.

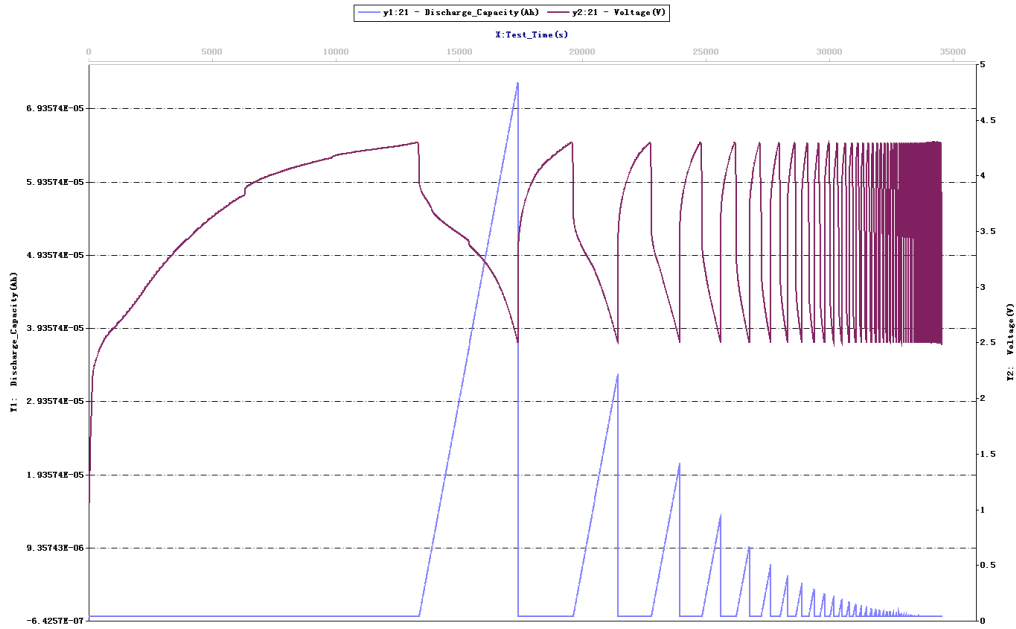


Figure 51: Discharge capacity (Blue) for the gap separator battery

4.4.4 Dripped Anode Using PGE

After successful charging and discharging was achieved using the gap separation method, the team tried implementing the PGE separator into the battery to make it possible to arrange the electrodes more closely together and improve energy density. Below in Figure 52 are the testing results for a battery produced by the dripped anode method utilizing the PGE separator.

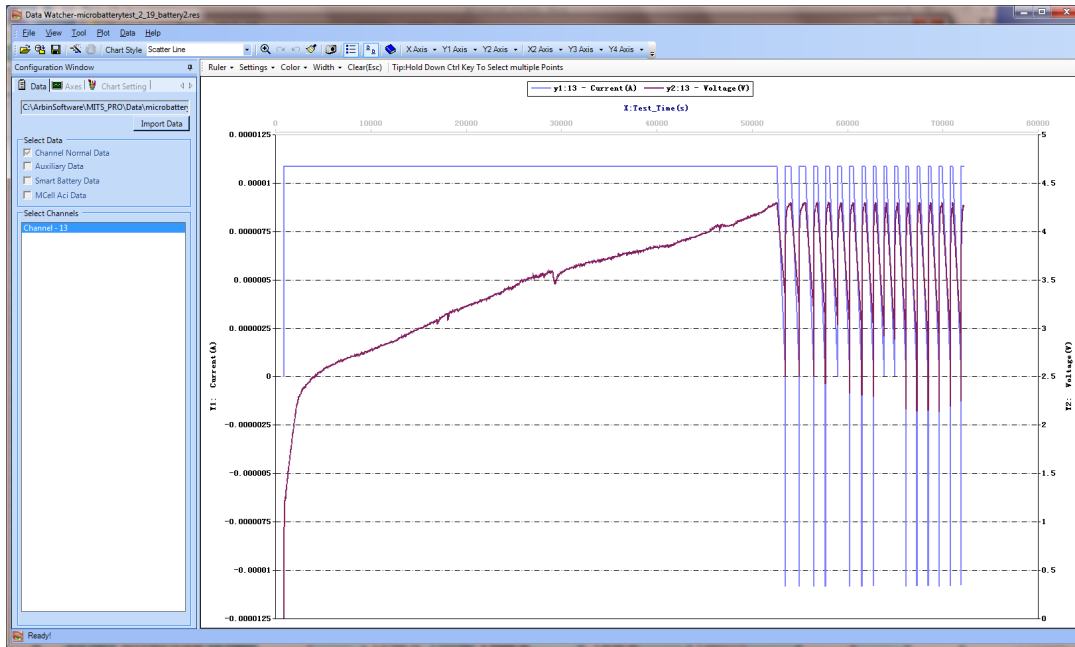


Figure 52: Results of battery test for dripped anode battery assembly method utilizing a PGE separator

The cell was able to charge to the expected voltage, which implies that there was no shorting. Unfortunately, the cell would not hold a charge or discharge capacity, and could not maintain its potential once charged.

The rapid charging and discharging observed during the later half of this test implied that there was too great of ionic resistance within the battery after initial charging had finished. Because ions could not easily flow from cathode to anode, a high electrical potential was almost instantly established as soon as charging began, instead of in a controlled manner as desired. This could have occurred for many reasons, including the decomposition or drying up of the electrolyte, incomplete saturation of the PGE separator, poor electrode structure, or a separator that was too thick for ions to be efficiently transported.

While we did not achieve success with this method of making our battery, development of the battery assembly and structure continues past the completion of this report. In future work, we will be building 2 more gap separator batteries to confirm our previous findings, as well as

continuing to build batteries with a PGE separator. Our next attempts at building the complete battery will involve altering the PGE separator thickness, and using other methods of saturating the PGE to ensure it is able to fully gel, and therefore provide better ion transport.

4.5 Challenges Associated With Micro-Battery

This project posed many challenges; primarily due to the size of the battery and its components. We assembled each cell by hand and as a result, many mistakes and imperfections were present in processing due to human error. These imperfections likely caused reduced performance of our battery. The two great challenges present in this process were developing a hermetic seal for the battery casing and the overall processing of the cell to build an operational battery.

4.5.1 Sealing the Battery

Sealing the battery was one of the major challenges of this project, as processing such a small cell by hand, while keeping the battery housing hermetic was quite cumbersome and difficult. One of our initial ideas was to use copper and aluminum circular plates as the current collectors. These plates would be slightly larger than the inner diameter of the glass tube. We would freeze the plates, insert them in the glass tubes and allow the plates to thermally expand; sealing the battery. Successfully implementing this strategy was difficult because we would have to ensure that the plates exerted enough thermal stress to seal the cell without breaking the glass. On doing more research, we discovered that Pyrex glass is not exactly circular which meant that some parts of the glass experience higher stresses than others. Due to this imbalance of stresses, we decided not to use the thermal expansion method.

Another method we discussed and tested was using copper and aluminum foil as the current collectors. We would simply cover one end of the glass tube with copper foil and we would cover the other end with aluminum foil. Once we covered both ends, we would adhere the foil to the glass with epoxy. As the batteries were so small, it was difficult to apply the epoxy to the glass and the foil while ensuring that none of the epoxy got into the battery, which could have contaminated the cell causing side reactions. Furthermore, had we sealed the cell using this method, it would be difficult to test the battery's performance because the smooth surface of the foil would have made it difficult to attach electrochemical testing leads to the cell.

We decided that for our application, the most suitable current collectors were metal rods. We bought aluminum dowel pins and copper rods which both had diameters that were comparable to the inner diameter of the glass tube. For more information on these current collectors, please see appendices E and F. The diameter of the aluminum dowel was slightly larger than the opening of the glass tube so we had to sand down the tip of the dowel pin to ensure a tight fit. We used a lathe to reduce the diameter of the copper rod and then sanded the tip if the rod still did not fit. Machining the copper was very difficult because copper is a soft metal and bends easily. Due to this characteristic, we had to cut the copper rod to a length of 6 – 8 inches before attempting to machine it.

Once both current collectors fit into the glass tube, we sealed the cell with Loctite epoxy. For more information this epoxy, please see Appendix G. We were worried that some of the epoxy would seep into the cell and that the seal may not be hermetic. To alleviate the latter concern, we conducted a test to determine how well we sealed each battery. The results of this test, mentioned above, proved that our sealing method was hermetic, and would be practical to implement for our batteries.

4.5.2 Processing the Cell

Along with the challenges of sealing the battery, we encountered several challenges while processing the cell. Initially we tried a solution stacking method of building the cell, where we sealed one end of cell, and then built the internal materials on top of one another before sealing the opposing end of the cell. For more information on this method see Appendix I. While inserting the active materials, it was very difficult to prevent air bubbles from forming, which created gaps and spaces in the electrodes and prevented precise injection and forming. After the active materials had been dried inside the cell, the components were pressed together using finger strength force applied to an aluminum peg. This additional compression led to many failed experiments as many glass tubes broke due to the additional stress.



Figure 53: Example of a battery housing breaking during processing

All final processing of the batteries had to occur in the argon glove box, which added further difficulty to processing. Working in the glove box with such small components was very difficult as the thick rubber gloves limited dexterity and our ability to handle the batteries. Sealing the battery housing was also difficult, as mixing the epoxy and carefully applying it

while preventing air bubbles from accumulating was cumbersome and had to be done in such a way that the rubber gloves were not damaged from the epoxy.

The greatest challenge of this project was finding a way to assemble the battery so that it would fully function, producing adequate charge and discharge capacity. Throughout testing of our batteries we encountered many issues such as short-circuiting, irregular charging, loss of potential after charging, and impedance of ion transfer. Many of these challenges have still not been overcome, causing us to have limited success in our battery development. While the short-circuiting and irregular charging issues were solved by changing the structure of the battery and using a gap separator method, several issues still remain. The greatest challenges that need to be overcome in order for our battery to be successful, are the ability of the battery to hold potential after charging and implementing the PGE separator in such a way that efficient ion transfer can occur. We predict that these issues are due to poor electrode structure and incomplete saturation and gelling of the PGE separator, although several unknown factors are likely present.

5.0 Conclusions & Recommendations

Throughout the duration of this project we learned many things about battery structure and chemistry, especially how these apply to batteries on the micro-scale. Starting from a basic glass cylinder, which was used as the battery housing, we were able to make significant progress in developing a micro lithium ion battery using simple, low-cost methods. Several methods of building a micro-battery were attempted and tested, and marginal success was achieved in producing a battery that could be charged and discharged. In this section we will draw conclusions from our research and testing during this project and offer recommendations for future work towards developing a micro-battery.

5.1 Conclusions from Battery Testing

Several variations of batteries were tested throughout this project with a wide range of failure and success. Our first battery prototypes built using the solution stacking method were plagued with inconsistency and short-circuiting. As the project progressed, we implemented a new method of building each electrode separately on its respective current collector, which improved electrode – current collector adhesion and eliminated incidents of short-circuiting. Additionally, an intermediary battery structure was tested using a physical spacing or “gap” between the electrodes, eliminating short-circuiting and potential issues with a PGE separator. This method made it difficult for minimal spacing between the electrodes to be achieved and limited the efficiency of our batteries, but allowed us to test the effectiveness of the other battery components, including the electrodes and current collectors.

While designed to be an intermediary step with hopes to lead to a complete battery featuring a PGE separator, the gap separator battery proved to be the most successful battery that

we produced. The success of the gap separator battery was recognized by its ability to charge and discharge for at least one cycle at a charging rate of $C/10$ (One tenth its theoretical charge capacity). No other battery that we produced throughout this project was able to accomplish this, while producing appreciable charge and discharge capacity. The most successful of our gap separator batteries was able to cycle approximately 3 times before losing appreciable charge and discharge capacity, and produced charge and discharge capacities of 0.243 mAh (35% of its theoretical maximum) and 0.0694 mAh (10% of its theoretical maximum) respectively. However it should be noted that these capacity values, especially the discharge capacity, were much lower than desired.

Attempts at producing a complete battery which featured a PGE separator, produced batteries that were not able to complete even one cycle of charging and discharging, although the issue short-circuiting of overcome by changing processing techniques and battery structure. It was predicted that several factors led to the failure and low efficiency of the batteries we developed during this project. These potential factors were: poor electrode structure, incomplete saturation and non-gelling of the PGE separator, water contamination in battery from processing, non-optimization of electrodes, and uneven distribution of the liquid electrolyte throughout the cell. Future work is required in order to over come these issues and produce a fully operational micro-battery with high energy density. While this team will continue to conduct testing and research until the completion of the academic year, additional work will most likely be required.

5.2 Recommendations for Future Work

The future of micro-battery technology lies in producing structures, which ensure safe and efficient internal battery operation while minimizing size and weight percentages of the

entire battery. Additionally, packaging needs to be developed that can hermetically seal the internal components of the battery and protect the battery from contamination and external factors such as UV radiation and applied stresses from processing and the demands of application. Such improvements may be found in utilizing other materials or other manufacturing methods. In the following section we will discuss some various parameters that can be optimized in future work.

5.2.1 Optimizing Current Packaging Design

We have proven that Pyrex Glass can sustainably provide an effective casing for Li-Ion battery operation. The Pyrex Glass cylinders, which we have been using, have a relatively large wall thickness in comparison to the overall volume of the cell. A minimum Pyrex Glass wall thickness that provides low enough permeability from exterior reactants for successful battery operation will need to be determined. Once a minimum is known, then an application specific wall thickness can be optimized so that the packaging will be able to withstand external factors along with environmental forces and loads. Along with reducing the wall thickness of the glass it is important to understand the minimum amount of epoxy needed for adequate sealing. By reducing the amount of epoxy used, the overall volume of the battery can be reduced. We believe that such optimizations can reduce the current volume of inactive materials by 50%.

5.2.2 Optimizing Current Processing Design

The battery production process that we have created to manufacture our micro-batteries is relatively primitive and lacks tolerance controls throughout. For future work, there is much improvement that can be made in our electrode and separator injection and sintering methods. First of all, a precision syringe should be utilized instead of a micropipette so that the amount of materials injected is more tightly controlled. Further research needs to be completed on the

ability of a simultaneous injection and sintering process to produce three-dimensional electrode architectures, which would improve energy density or power density. By creating a process which allows us to engineer specific 3D electrode structures we may be able to solve the issue of poor capacity retention. Ideally, this entire process should be automated to minimize human error, but this would not be necessary until more research and development is conducted.

5.2.3 Mold Materials and Manufacturing Techniques

The current mold of our battery is Pyrex Glass due to its electrochemical stability. It is limited in size reductions due to its minimal process ability. It is important to overview other mold materials that can be formed to create an optimum market-worthy micro-lithium ion battery. In the following sections we will discuss various materials and manufacturing techniques for future mold designs.

Glasses and Ceramics

There are inherent disadvantages in using glass or ceramics as a packaging material for a micro-battery or any application. Although ceramics and glasses have relatively high mechanical strength, they are very brittle and thus shatter under certain load conditions. This attribute restricts the assembly process of the cell along with the functional environments that the batteries can be exposed to. Another downfall is that there is limited manufacturability in making complex designs. One advantage is that glasses and some ceramics have low permeability, which makes them highly suitable in blocking external reactants from entering the cell.

Metals

Metals are comparable in strength and permeability to ceramic and glasses but have the advantage of greater ductility. This improves manufacturability along with impact toughness during application usage. A major issue with metals is that many metals react with active battery

materials and are not suitable to be directly in contact with the electrodes. Usually a thin layer of non-reactive material is placed between the exterior metal packaging and the active materials. This method intrinsically requires the use of extra inactive materials to ensure proper operation, adding to the volume of the battery and reducing energy density.

Polymers

Polymers generally have lower mechanical strengths than ceramics and metals but are usually superior in ductility. Polymers can be manufactured to have a wide variety of material properties and also into complex forms. Due to the wide array of polymers available it is necessary to conduct more research into the feasibility of integrating them with battery packaging. Some fundamental issues include high permeability, which allows reactants to flow through the pores of the polymer and could negatively affect battery operation. Some polymers that hold great potential in meeting the mechanical and reactive criteria's of an efficient battery packaging include: Teflon, high density polyethylene (HDPE), and PMMA. There is great potential in dip coating battery components with such polymers to produce thin evenly distributed covers for the battery. Our team encourages future research and development to focus on the potential of utilizing various polymers or polymer-metal composites in producing optimal micro-battery casings.

References

- Agrawal, R. C., & Pandey, G. P. (2008). Solid polymer electrolytes: materials designing and all-solid-state battery applications: an overview. *Journal of Physics D: Applied Physics*, *41*(22), 223001.
- Anderson, H. L., Jones, F. R., & Wood, R. H. (1964). A simple method of coating with polyethylene. *Journal of Chemical Education*, *41*(12), 638.
- Anode Active Materials. Retrieved December 26, 2014, from <http://www.targray.com/li-ion-battery/anode-materials/anode-active-materials>
- Arthur, T., Bates, D., Cirigliano, N., Johnson, D., Malati, P., Mosby, J., ... Dunn, B. (2011). Three-dimensional electrodes and battery architectures. *MRS Bulletin*, *36*, 523-531.
- Bates, M. (2012). HOW DOES A BATTERY WORK? Retrieved January 28, 2015, from <http://engineering.mit.edu/ask/how-does-battery-work>
- Battery Anodes. (2014). *The Energy Materials Center at Cornell Site* Retrieved October 20, 2014, from <http://www.emc2.cornell.edu/content/view/battery-anodes.html>
- Battery Cathodes. (2014). *The Energy Materials Center at Cornell Site* Retrieved October 21, 2014, from <http://www.emc2.cornell.edu/content/view/battery-cathodes.html>.
- Braithwaite, J. W., Gonzales, A., Nagasubramanian, G., Lucero, S. J., Peebles, D. E., Ohlhausen, J. A., et al. (1999). Corrosion of Lithium-Ion Battery Current Collectors. *Journal of The Electrochemical Society*, *146*(2), 448-456.
- BU-101: When Was the Battery Invented? *Information on the Invention of the Battery* Retrieved October 27, 2014, from http://batteryuniversity.com/learn/article/when_was_the_battery_invented.
- BU-301a: Types of Battery Cells. (2015, 2/11/2015). Retrieved 2/15, 2015, from http://batteryuniversity.com/learn/article/types_of_battery_cells
- Buchmann, I. (2001). When Was the Battery Invented? Retrieved October 28, 2014, from <http://www.buchmann.ca/article3-page1.asp>
- Bullis, K. (2013). Battery Material Prevents Fires, Stores Five Times the Energy.
- Capozzo, D., Fleming, S., Foley, B., & Macri, M. (2006). Lithium Ion Battery Safety.
- Carnegie, R., Gotham, D., Nderitu, D., & Preckel, P. (2013). Utility Scale Energy Storage Systems: Benefits, Applications, and Technologies

- Chan, C., Peng, H., Liu, G., McIlwrath, K., Zhang, X. F., Huggins, R., et al. (2007). High-performance Lithium Battery Anodes Using Silicon Nanowires. *Nature Nanotechnology* 3, 31 - 35.
- Chandra, D., Chien, W.-M., & Talekar, A. Metal Hydrides for NiMH Battery Applications. Retrieved January 28, 2015, from <http://www.sigmaldrich.com/technical-documents/articles/material-matters/metal-hydrides-for.html>
- Downs, D., & Meyeroff, A. Smith College Museum of Ancient Inventions: Baghdad Battery. *Smith College Museum of Ancient Inventions: Baghdad Battery* Retrieved October 28, 2014, from http://www.smith.edu/hsc/museum/ancient_inventions/battery2.html
- Fergus, J. (2010). Recent Developments in Cathode Materials for Lithium Ion Batteries. *Journal of Power Sources* 195, 939-954.
- Golodnitsky, D., Yufit, V., Nathan, M., Shechtman, I., Ripenbein, T., Strauss, E., ... & Peled, E. (2006). Advanced materials for the 3D microbattery. *Journal of Power Sources*, 153(2), 281-287.
- Gowda, S. R., Reddy, A. L. M., Shaijumon, M. M., Zhan, X., Ci, L., & Ajayan, P. M. (2010). Conformal coating of thin polymer electrolyte layer on nanostructured electrode materials for three-dimensional battery applications. *Nano letters*, 11(1), 101-106.
- Hammel, C., Ring, S., & Vimmerstedt, L. (1995). Current Status of Environmental, Health, and Safety Issues 151 of Lithium Ion Electric Vehicle Batteries.
- King, W., Braun, P., Cho, J., Zhang, H., & Pikul, J. (2013). High-power lithium ion microbatteries from interdigitated three-dimensional bicontinuous nanoporous electrodes. *Nature Communications*, 1732.
- Lai, W., Erdonmez, C. K., Marinis, T. F., Bjune, C. K., Dudney, N. J., Xu, F., et al. (2010). Ultrahigh-Energy-Density Microbatteries Enabled by New Electrode Architecture and Micropackaging Design. *Advanced Materials*, 22(20), E139-E144.
- Madison, N. What Is an Electrode. *WiseGEEK* Retrieved October 19, 2014, from <http://www.wisegeek.org/what-is-an-electrode.htm>
- Marshall, B., Brayant, C., & Pumphrey, C. How Batteries Work. Retrieved January 28, 2015, from <http://electronics.howstuffworks.com/everyday-tech/battery5.htm>
- McKissock, B., Loyselle, P., & Vogel, E. (2009). Guidelines on Lithium-ion Battery Use in Space Applications Glenn Research Center, Cleveland, Ohio.
- Nasybulin, E., Xu, W., Engelhard, M., Nie, Z., Li, X., & Zhang, J.-G. (2013). Stability of polymer binders in Li-O₂ batteries. *Journal of Power Sources*, 899-907.

- Niitani, T., Shimada, M., Kawamura, K., & Kanamura, K. (2005). Characteristics of new-type solid polymer electrolyte controlling nano-structure. *Journal of power sources*, 146(1), 386-390.
- OLTEAN, G. (2014). Aluminium Rod Structures for Three-dimensional Li-ion Micro-battery Applications. ACTA UNIVERSITATIS UPSALIENSIS UPPSALA
- Orendorff, C. J. (2012). The role of separators in lithium-ion cell safety. *Electrochemical Society Interface*, 21(2), 61-65.
- Panasonic Commercializes the Industry's Smallest Pin Shaped Lithium Ion Battery. (2014). Retrieved 2/15, 2015, from <http://news.panasonic.com/press/news/official.data/data.dir/2014/10/en141003-2/en141003-2.html>
- Rechargeable Coin Batteries: NBL Series. Retrieved 2/15, 2015, from <http://na.industrial.panasonic.com/products/batteries/rechargeable-batteries/rechargeable-coin/series/nbl-series/CS523?reset=1>
- Ren, J., Li, L., Chen, C., Chen, X., Cai, Z., Qiu, L., et al. (2013). Twisting Carbon Nanotube Fibers for Both Wire-Shaped Micro-Supercapacitor and Micro-Battery. *Advanced Materials*, 25(8), 1155-1159.
- Safety Hazards of Batteries. Retrieved December 27, 2014, from http://www.nrel.gov/education/pdfs/lithium-ion_battery_safety_hazards.pdf
- Sharp, I. (2010). Electronics for Absolute Beginners.
- Shin, H. C., & Liu, M. (2005). Three-Dimensional Porous Copper–Tin Alloy Electrodes for Rechargeable Lithium Batteries. *Advanced Functional Materials*, 15(4), 582-586.
- Sun, K., Wei, T. S., Ahn, B. Y., Seo, J. Y., Dillon, S. J., & Lewis, J. A. (2013). 3D Printing of Interdigitated Li-Ion Microbattery Architectures. *Advanced Materials*, 25(33), 4539-4543.
- Tarascon, J. M., & Armand, M. (2001). Issues and challenges facing rechargeable lithium batteries. *Nature*, 414(6861), 359-367.
- THE COPPER ADVANTAGE*. Antimicrobial Copper.
- Trends in cathode material for Li-ion secondary batteries. Retrieved December 27, 2014, from http://www.sneresearch.com/eng/info/show.php?c_id=4960&pg=6&s_sort=&sub_c at=&s_type=&s_word=
- Wang, L. (2012). SOLID ELECTROLYTES FOR NEXT GENERATION BATTERIES.

- Whitehead, A. H., & Schreiber, M. (2005). Current collectors for positive electrodes of lithium-based batteries. *Journal of The Electrochemical Society*, 152(11), A2105-A2113.
- Whittingham, S. (2004). Lithium Batteries And Cathode Materials. *Chemical Reviews* 104, 4271-4302.
- Xu, K. (2004). Nonaqueous liquid electrolytes for lithium-based rechargeable batteries. *Chemical reviews*, 104(10), 4303-4418.
- Zhang, H. P., Zhang, P., Li, Z. H., Sun, M., Wu, Y. P., & Wu, H. Q. (2007). A novel sandwiched membrane as polymer electrolyte for lithium ion battery. *Electrochemistry communications*, 9(7), 1700-1703.
- Zhang, J., Sun, B., Huang, X., Chen, S., & Wang, G. (2014). Honeycomb-like porous gel polymer electrolyte membrane for lithium ion batteries with enhanced safety. *Scientific reports*, 4.
- Zhao, M., Kariuki, S., Dewald, H. D., Lemke, F. R., Staniewicz, R. J., Plichta, E. J., et al. (2000). Electrochemical Stability of Copper in Lithium-Ion Battery Electrolytes. *Journal of the Electrochemical Society*, 147(8), 2874-2879.
- Zhu, Y. Thick-Walled Cylinders, *MAE 316 – Strength of Mechanical Components*.

Appendices

Appendix A: Summary of Historical discoveries

Table 4: Summary of Historical Findings

Year	Inventor	Discovery
1600	William Gilbert (UK)	Establishment of electrochemistry study
1745	Ewald George von Kleist (Netherlands)	Invention of Leyden jar. Stores static electricity
1791	Luigi Galvani (Italy)	Discovery of “animal electricity”
1800	Alessandro Volta (Italy)	Invention of the voltaic cell (zinc, copper disks)
1802	William Cruickshank (UK)	First electric battery capable of mass production
1820	André-Marie Ampère (France)	Electricity through magnetism
1833	Michael Faraday (UK)	Announcement of Faraday’s law
1836	John F. Daniell (UK)	Invention of the Daniell cell
1839	William Robert Grove (UK)	Invention of the fuel cell (H ₂ /O ₂)
1859	Gaston Planté (France)	Invention of the lead acid battery
1868	Georges Leclanché (France)	Invention of the Leclanché cell (carbon-zinc)
1899	Waldmar Jungner (Sweden)	Invention of the nickel-cadmium battery
1901	Thomas A. Edison (USA)	Invention of the nickel-iron battery
1932	Shlecht & Ackermann (Germany)	Invention of the sintered pole plate
1947	Georg Neumann (Germany)	Successfully sealing the nickel-cadmium battery
1949	Lew Urry, Eveready Battery	Invention of the alkaline-manganese battery
1970s	Group effort	Development of valve-regulated lead acid battery
1990	Group effort	Commercialization of nickel-metal-hydride battery
1991	Sony (Japan)	Commercialization of lithium-ion battery
1994	Bellcore (USA)	Commercialization of lithium-ion polymer
1996	Moli Energy (Canada)	Introduction of Li-ion with manganese cathode
1996	University of Texas (USA)	Identification of Li-phosphate (LiFePO ₄)
2002	University of Montreal, Quebec Hydro, MIT, others	Improvement of Li-phosphate, nanotechnology, commercialization

Appendix B: Targray's Portfolio of Graphite Active Materials

Table 5: Targray's Portfolio of Graphite Active Materials

Product Series	Characteristics		Discharge Capacity	First Efficiency	Design Capacity / Full Cell	D ₅₀	BET	Tap Density
			mAh/g	%	mAh/g	um	m ² /g	g/cm ³
High Performance Anode Material	Compound natural graphite, high capacity, high first efficiency, good machinability	PGPT100	365.2	95.1	345-355	18-21	1.68	≥1.15
	High performance artificial graphite, high capacity, high rate capability, good cycle/ safety performance	PGPT200	338.52	94.5	325-335	23-27	0.92	≥1.08
		PGPT202	340.3	94.5	325-335	13-17	2	≥0.95
Anode material for power cell	High rate capability material	PGPT300	343.1	93.9	352-330	20-24	1.68	≥1.05
		PGPT301	343.2	93	320-325	13-17	2.09	≥0.90
	Capacity-type anode material for power cell	PGPT350	327	90.2	295-305	22-26	4.8	≥1.15
		PGPT351	342.4	90.8	320-330	21-25	5.2	≥0.90
Anode Material	Modified natural graphite, high capacity, good machinability	PGPT400	361.6	94.2	340-345	18-20	1.86	≥1.05
		PGPT405	>355.3	92.1	342-350	41926	<3.0	>1.1
	Graphite conductive additives	PGPT501	350	83	3	9	20	10.8

Appendix C: A Comparison of Various Cathodes

Table 6: A Comparison of Various Cathode Materials

	LiCoO_2	LiNiO_2	LiMn_2O_4	LiFePO_4
Theoretical Capacity (mAh/g)	274	274	148	170
Practical Capacity	120~155	135~180	100~130	100~160
Rate capability	Good	Medium	Poor	Poor
Cycle Life	Good	Good	Fair	Good
Operating Voltage (vs. Li/Li^+)	3.9	3.8	4.1	3.4
High temperature property	Good	Good	Poor	Good
Thermal stability	Poor	Very poor	Good	Good
Density (g/cm^3)	5.1	4.8	4.2	3.6
Environment	Toxic	Toxic	Green	Green
Cost (\$/kg)	25	13	0.5	0.23
Synthesis	Easy	Hard	Tricky	Hard

Cost of Individual cathode components

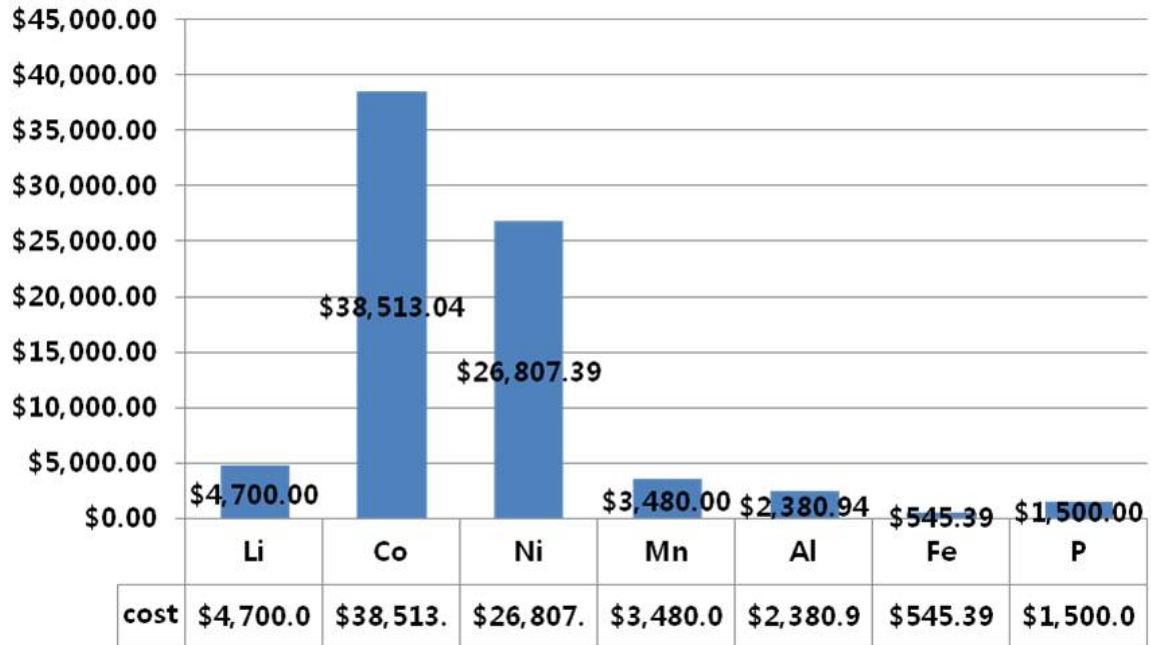


Figure 54: Cost of Individual cathode components

Appendix D: Safety Hazards of Batteries

Battery technology is at the heart of much of our technological revolution. One of the most prevalent rechargeable batteries in use today is the Lithium-ion battery. Cell phones, laptop computers, GPS systems, iPods, and even cars are now using lithium ion rechargeable battery technology. In fact, you probably have a lithium-ion battery in your pocket or purse right now.

Although lithium-ion batteries are very common there are some inherent dangers when using ANY battery. Lithium cells are like any other technology – if they are abused and not used for their intended purpose catastrophic results may occur, such as: first-, second-, and third-degree burns, respiratory problems, fires, explosions, and even death. Please handle the lithium-ion batteries with care and respect.

User Safety Precautions

Short-Circuiting

- When the battery is not in use, you **MUST** disconnect the battery from the battery connector. When the battery is connected to the battery connector, do not leave unattended since the two wires with the alligator clips can touch which will heat up the battery. Short-circuiting will damage the battery and generate heat that can cause burns.
- Don't leave the battery in the charger once it is fully charged. The battery charger will flash on and off with a red indicator light every 20 seconds when the battery is fully charged. Overcharging the batteries will not increase the performance and could lead to damage.

Disassembly

- Never disassemble a battery as the materials inside may be toxic and may damage skin and clothes.
- DO NOT place a battery in fire; this may cause the battery to rupture. The electrolyte is very flammable and if an ignition source exists, then fire and even an explosion could result.
- NEVER place batteries in water, as this may cause the battery to rupture and release poisonous gasses. Furthermore, when the electrolyte is combined with water, there is the potential for hydrofluoric acid to form – an extremely toxic and corrosive substance.

Soldering

- Never solder anything directly to a battery. This can destroy the safety features of the battery by damaging the safety vent inside the cap.

Charging

- Never charge with an unspecified charger or specified charger that has been modified. This can cause breakdown of the battery or swelling and rupturing.
- Never attempt to charge a battery which has been physically damaged.
- Avoid designing airtight battery compartments. In some cases, gases (oxygen, hydrogen) may be given off, and there is a danger of a battery bursting or rupturing if ignited by sparks.
- Do not use a battery in an appliance or purpose for which it was not intended.

Safety Procedures

- If the foil packaging on the battery does break, vent the room and leave area.

- If a fire starts, call the fire department immediately. The only extinguisher that will work on a Lithium-ion Battery fire is a Class D Fire Extinguisher or Dry Sand or Dry Table Salt.

Battery Disposal

Lithium-ion batteries are found in many electronics like laptops, digital cameras, power tools, and cordless phones. These batteries are very popular because they can be recharged and because they are able to supply power for a long period of time. However, even lithium-ion batteries reach a point where they can no longer hold a charge and need to be disposed of. When this time comes, it is important to know how to recycle the battery, and not simply put it in a trash can.

There are many reasons to recycle these batteries rather than throw them away where they may end up in a regular landfill. This is because they enter the solid waste stream and can contaminate soil and water.

Externally Short Circuit Cell

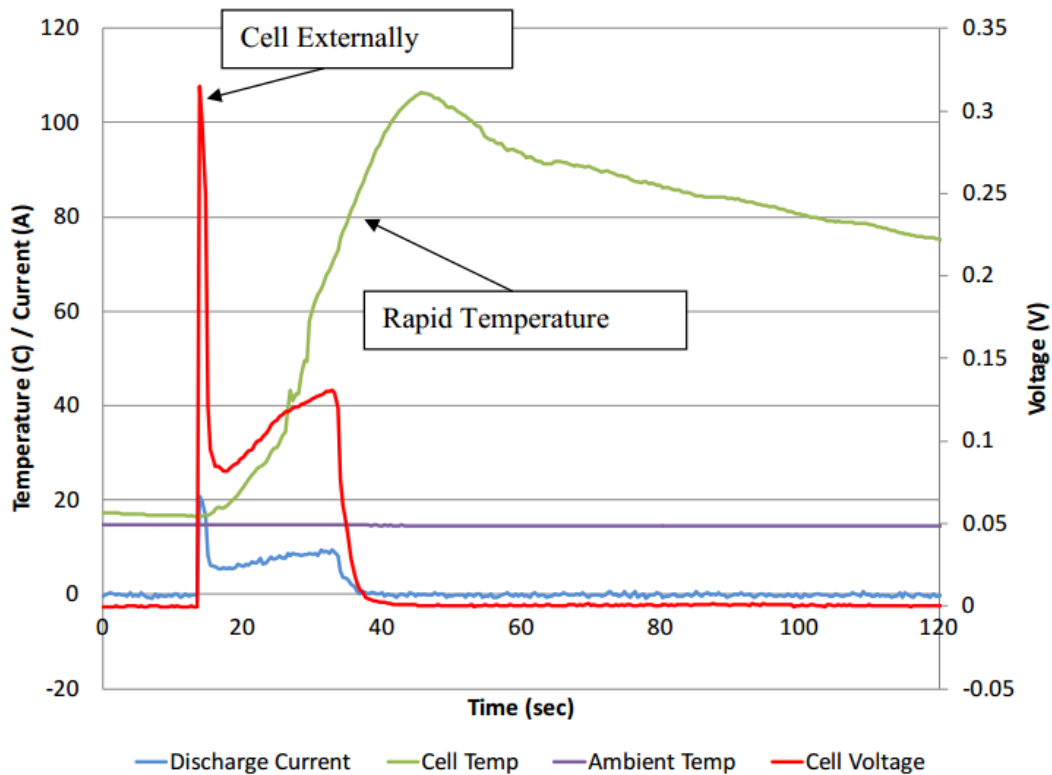


Figure 55: Externally short-circuited cell

- After the cell was externally shorted (akin to dropping a wrench across the positive and negative terminals), the temperature of the cell rose to approximately 106° C (223° F).
- The excessive temperatures within the cell caused the electrolyte to internally vaporize; this, in turn, pressurized the aluminum packaging material of the battery.
- After pressurization, the aluminum packaging vented out of the bottom of the cell and liquid electrolyte was seen on the test surface.
- Smoke also exited the vent hole but a fire did not result.
- The current draw from the battery exceeded the 12C rating of the cell by a factor of 10

Appendix E: Aluminum Current Collector Information



Figure 56: Aluminum dowel pin

Easier to machine than standard dowel pins, these multipurpose, low-strength pins have at least one beveled end to aid insertion. They are slightly oversized for a tight fit.

Aluminum is one third lighter than steel. It is corrosion resistant and it has good thermal and electrical conductivity.

Diameter tolerance is +0.0001" to +0.0003".

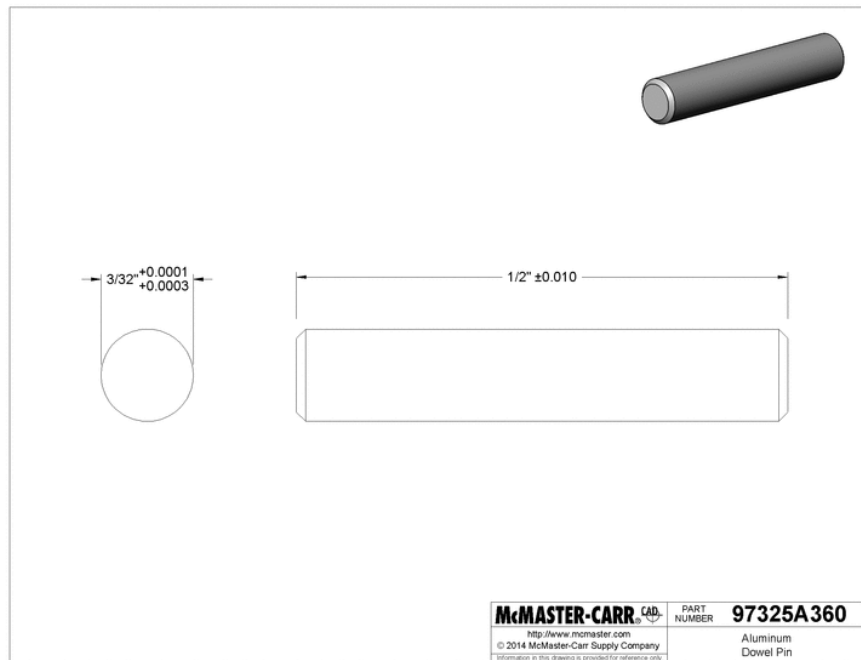


Figure 57: Drawing of the dowel pin

Chart of Aluminum Properties

Table 7: Chart of Aluminum Properties

Alloy	Temper	Ultimate Tensile Strength, ksi	Yield Strength, ksi	Elongation %in ²	Brinell Hardness	Shear Strength, ksi	Thermal Conductivity @ 77° F (BTU/ft ² /in./hr.)	Electrical Conductivity @ 68° F (% of Intl. Copper Standard)	Electrical Resistivity @ 68° F (Ohm -Cir. Mil/ft.)	Nominal Density (lbs./cu. in.)
1100	O	13	5	35	23	9	1540	59	18	0.098
	H14	18	17	9	32	11	1510	57	18	0.098
	H18	24	22	5	44	13	1510	57	18	0.098
2011	T3	55	43	n/a	95	32	1050	39	27	0.102
2017	O	26	10	n/a	45	18	1340	50	21	0.101
	T4, T451	62	40	n/a	105	38	930	34	31	0.101
2024	O	27	11	20	47	18	1340	50	21	0.1
	T3	70	50	18	120	41	840	30	35	0.1
	T4, T351	68	47	20	120	41	840	30	35	0.1
3003	O	16	6	30	28	11	1340	50	21	0.099
	H14	22	21	8	40	14	1100	41	25	0.099
	H18	29	27	4	55	16	1070	40	26	0.099
4032	T6	55	46	n/a	120	38	960	35	30	0.097
5052	O	28	13	25	47	18	960	35	30	0.097
	H32	33	28	12	60	20	960	35	30	0.097
	H38	42	37	7	77	24	960	35	30	0.097
6013	T8	65	62	11	130	36	1140	38	n/a	0.098
6020	T8	44	42	15	100	n/a	1190	46	n/a	0.098
6061	O	18	8	25	30	12	1250	47	22	0.098
	T6, T651	45	40	12	95	30	1160	43	24	0.098
		45	40	12	95	30	1160	43	24	0.098
6063	O	13	7	n/a	25	10	1510	58	18	0.097
	T5	27	21	12	60	17	1450	55	19	0.097
	T83	37	35	9	82	22	1390	53	20	0.097
6262	T9	58	55	n/a	120	35	1190	44	24	0.098
7068	T6511	103	99	9	190	53	n/a	30	n/a	0.103
7075	O	33	15	17	60	22	n/a	n/a	n/a	0.101
	T6	83	73	11	150	48	900	33	31	0.101
	T651	83	73	11	150	48	900	33	31	0.101

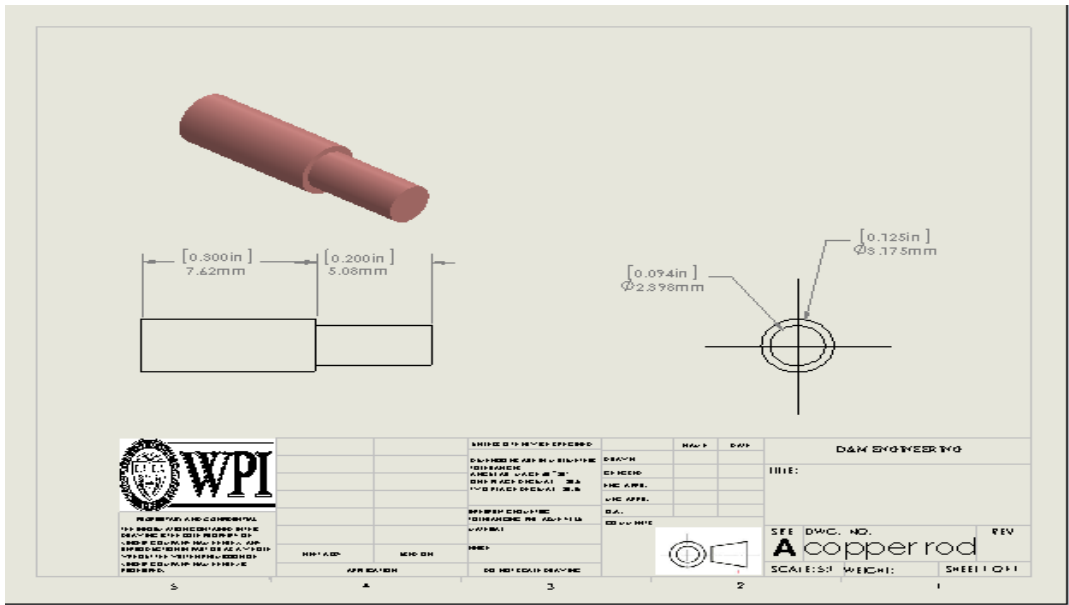


Figure 59: Drawing of the copper rod

Table 8: Chart of Copper Alloy Properties

Copper and Copper Alloy		Test Temperature, K	Plastic Properties			
No.	Name and Treatment		Uniaxial			
			Tensile Strength, psi	Yield Strength, psi	Elongation, % in 4D	Reduction of Area, %
102	Oxygen Free (Cold drawn 60%)	295	48,400	46,800	17	77
		195	52,900	49,800	20	74
		76	66,400	54,400	29	78
		20	74,500	58,500	42	76
		4	74,600	58,600	41	75
122	Phosphorus Deoxidized, High Residual Phosphorus (Annealed)	295	31,300	6,700	45	76
		195	38,300	6,600	56	87
		76	50,600	7,400	62	84
		20	63,800	8,400	68	83
		4	60,400	7,900	65	81
	(Cold drawn 26%)	295	51,800	49,400	17	76
		195	56,800	53,600	21	79
		76	68,400	59,900	28	76
		20	81,400	64,100	46	78
		4	81,000	63,600	44	72
150	Zirconium Copper (Cold drawn, aged)	295	64,450	59,600	16	62
		195	67,200	61,300	20	66
		76	77,400	65,700	26	71
		20	85,200	66,400	37	72
		4	85,700	64,700	36	69
220	Commercial Bronze, 90% (Annealed)	295	38,500	9,600	56	84
		195	41,800	10,200	57	80
		76	55,200	13,200	86	78
		20	73,200	15,600	95	73
		4	68,200	15,000	91	73
230	Red Brass, 85% (Cold drawn)	295	40,400	13,000	48	74
		195	46,500	14,000	63	79
		76	62,000	16,400	83	77

	14%)	20	79,200	20,900	80	75
		4	71,000	18,300	82	71
443	Admiralty Arsenical (Annealed)	295	44,800	10,600	86	81
		195	49,600	12,600	91	79
		76	64,600	18,700	98	73
		20	76,800	20,800	99	68
		4	78,600	21,100	92	72
464	Naval Brass (Annealed)	295	63,300	31,000	37	52
		195	67,400	33,800	37	54
		76	80,400	38,000	44	48
		20	105,200	47,600	41	42
		4	99,600	43,700	40	48
510	Phosphor Bronze, 5% A (Cold drawn 85%, spring)	295	77,400	72,000	18	78
		195	85,600	78,700	20	78
		76	105,200	89,200	34	67
		20	131,000	104,800	39	62
		4	116,400	100,400	34	58
614	Aluminum Bronze D (Annealed)	295	83,200	59,400	40	66
		195	89,500	64,800	45	71
		76	105,800	69,500	52	64
		20	126,400	80,600	48	58
		4	134,500	82,400	52	59
647	Copper-Nickel Silicon (Aged)	295	112,400	105,000	15	60
		195	119,400	110,800	18	66
		76	123,600	114,100	24	70
		20	133,700	118,400	33	68
		4	135,800	119,800	31	65
655	High Silicon Bronze A (Annealed, soft)	295	61,400	24,200	66	79
		195	69,900	26,800	68	79
		76	89,000	31,900	71	69
		20	108,900	37,600	72	69
		4	101,200	36,900	71	70
706	Copper Nickel 10% (Annealed)	295	49,600	21,400	37	79
		195	54,700	24,700	42	77
		76	72,000	24,800	50	77
		20	82,500	30,200	50	73
		4	80,600	24,900	53	73
715	Copper Nickel 30% (Annealed)	295	57,800	18,700	47	68
		195	68,000	22,200	48	70
		76	89,800	31,600	52	70
		20	103,100	38,100	51	66
		4	104,600	40,100	48	65
	Nickel- Aluminum Bronze (Sand cast)	295	101,200	44,000	11	9
		195	104,600	47,800	9	9
		76	117,100	54,900	6	7
		20	126,600	61,600	6	2
		4	130,500	60,100	6	5

Appendix G: Epoxy Specifications



Figure 60: Loctite epoxy

This epoxy is a two part adhesive consisting of an epoxy resin and a hardener. When both parts are mixed in equal volumes, the resin and hardener react to produce a tough, rigid, high strength bond in 5 minutes for most projects. This product is available in a convenient dual syringe which delivers equal parts of both components every time. This epoxy can be used as an adhesive for a wide range of materials or as a versatile filler for gap filling, surface repairs and laminating. The epoxy does not shrink and is resistant to water and most common solvents. It can be tinted with earth pigments, cement or sand for color matching. It can be sanded and drilled.

Table 9: Features and Benefits of Epoxy

Feature	Benefit
High impact resistance	Won't crack when drilled
Can be tinted	Matches surrounding materials
Water resistant	Can use outdoors
Will not shrink	One-time application
Convenient double syringe	Dispenses equal amounts of each component every time
Sets in 5-10 minutes	Quick completion of project

Tools Typically Required:

Utility knife, mixing tool/applicator (e.g. wooden stick) and disposable surface (e.g. foil or paper cup).

Safety Precautions:

Apply in a well ventilated area. Wear gloves and wash hands after use.

Preparation:

Surfaces must be clean, dry and free from oil, wax and paint. Roughen smooth surfaces for better adhesion by sandblasting or sanding with emery cloth. Wash glass and ceramic surfaces with soap and water then rinse and let dry. Pre-fit parts to be joined. Remove the plug from between the piston. Cut off the end tips of the syringe. Turn syringe end up and pull plunger back slightly allowing air bubbles to rise to top. Press plunger to expel air. Depress the double piston to dispense equal parts of the two materials on a disposable surface. Wipe syringe tips clean, retract piston slightly and close with the plug. Ensure that the plug is always placed in the same orientation on the tips. Mix resin and hardener for one minute thoroughly.

Application:

For best results apply a small amount of mixed adhesive to both surfaces within one to two minutes of mixing and press together. Placing parts together close to the 5 minute set time will reduce adhesion. Remove any excess glue immediately with acetone. Support bond for 10 minutes at room temperature. Usable strength achieved in 1 hour. Fully cured in 24 hours.

Clean-up:

Clean excess glue immediately by wiping with clean cloth. Acetone may be used to assist in removal. Cured adhesive may be cut away with caution using a sharp blade. Prolonged immersion in paint stripper will soften the cured adhesive to aid removal. Note: Acetone is

highly flammable and not compatible with all surfaces. Follow manufacturer's instructions and test on small area before applying.

Typical Uncured Physical Properties

Color:

Hardener: Light yellow

Resin: Colorless

Base:

Epoxy resin / Polymercaptan hardener

Specific Gravity:

Hardener: 1.04

Resin: 1.17

Flash Point:

Hardener: >200°F (93°C)

Resin: > 480°F (249°C)

VOC Content:

(Resin & Hardener) 0.1% by weight

Shelf Life:

24 months from date of manufacture

(unopened)

Typical Application Properties

Application Temperature:

39°F (4°C) to 95°F (35°C)

Odour:

Amine

Gel Time:

(5 g : 5g)

4 to 10 minutes (Gel time is dependent upon temperature and the amount of adhesive used)

Usable Strength: 1 hour

Full Cure Time: 24 hours

Typical Cured Performance Properties

Color: Clear to amber

Service Temperature:

Long Term Exposure: -9°F(-23°C) to 120°F(49°C)

Short Term Exposure: -9°F(-23°C) to 302°F(150°C)

Water Resistant: Yes

Sandable: Yes

Paintable: No but can be tinted using earth pigments, cement or sand

Tensile Shear Strength:

Cold Rolled Steel, Sandblasted

1 hour: 1322 ± 128 psi (9.11 ± 0.88 N/mm²)

4 hours: 2494 ± 78 psi (17.20 ± 0.54 N/mm²)

24 hours: 3437 ± 58 psi (23.70 ± 0.40 N/mm²)

7 days: 3426 ± 155 psi (23.62 ± 1.07 N/mm²)

Aluminum, Sandblasted, 24 hours: 2055 ± 290 psi (14.17 ± 2.0 N/mm²)

Compression Shear Strength – 24 hours:

Hard PVC (White), Sanded: 1081 ± 199 psi (7.45 ± 1.37 N/mm²)

Acrylite FF, Sanded: 958 ± 268 psi (6.61 ± 1.85 N/mm²)

Maple: 2088 ± 243 psi (14.40 ± 1.68 N/mm²)

Water Resistance – Tensile Shear Strength:

(Aluminum, Sandblasted, 7 day cure)

Followed by 7 day Water Immersion: 2048 ± 160 psi (14.12 ± 1.10 N/mm²)

Solvent Resistance - Tensile Shear Strength:

(Aluminum, Sandblasted, 7 day cure)

Followed by 24 hour Gasoline Immersion: 3216 ± 275 psi (22.17 ± 1.90 N/mm²)

Side Impact Resistance:

(Cold Rolled Steel, Sandblasted, 1"x1", 7 day cure) 6.8 Joules

Appendix H: Pyrex Glass Technical information

Chemical Resistance

Borosilicate glass is inert to almost all materials with the exception of hydrofluoric acid, hot phosphoric acid and hot alkalis. Of these, hydrofluoric acid has the most serious effect and, even when a solution contains a few parts per million, attack will occur.

Phosphoric acid and caustic solutions cause no problems when cold but at elevated temperatures corrosion occurs. Caustic solutions up to 30% concentration can be handled safely at ambient temperatures.

Physical Properties:

Composition

Low-expansion borosilicate glass has the following approximate chemical composition:

SiO ₂	81%
Na ₂ O	4.0%
K ₂ O	0.5%
B ₂ O ₃	13.0%
Al ₂ O ₃	2.0%

Linear Coefficient of Expansion:

Between 32°F and 572°F [0°C and 300°C], per ASTM Method E 228)

18.1×10^{-7} in/in/7°F / 32.5×10^{-7} cm/cm/°C

Annealing:

All fittings and all straight lengths are annealed to reduce internal stress. This also makes the pipe easier to field fabricate.

Thermal Conductivity:

0.73 Btu/hr-ft²-°F/ft

0.0035 cal/sec-cm²-°C/cm

Specific Heat:

0.20 Btu/lb-°F

0.20 cal/gm-°C

Dielectric Constant:

At 23°C and 1M Hz per ASTM Method D 150:

4.6 ±0.2

Density:

Approximately 139 lb/ft³ (2.23 gm/cm³)

Young's Modulus: per ASTM Method C215:

Ranges from 9 x 10⁶ to 10 x 10⁶ psi. (64GPa)

Mechanical Strength:

The mechanical properties of glass differ from those of metals. The lack of ductility of glass prevents the equalization of stresses at local irregularities or flaws and the breaking strength varies considerably about a mean value. This latter is commonly found to occur at a tensile strength of about 70 kg/ cm² (1000 psi). The glass should be adequately supported and appropriate allowance should be made for special conditions such as high temperatures, dense liquids, etc.

Working Temperatures

Borosilicate glass retains its mechanical strength and will deform only at temperatures which approach its strain point. The practical upper limit for operating temperatures is much

lower and is controlled by the temperature differentials in the glass, which depend on the relative temperatures of the contents of the equipment and the external surroundings.

Provided borosilicate glass is not subjected to rapid change in temperature, creating undue thermal shock, it can be operated safely at temperatures up to 450°F (232°C). The normal limiting factor is actually the gasket material. The degree of thermal shock (usually defined as sudden chilling) which it can withstand depends on many factors, for example: stresses due to operating conditions; stresses imposed in supporting the equipment; the wall thickness of the glass, etc. It is therefore undesirable to give an overall figure but, as a general guide, sudden temperature changes of up to about 216°F (120°C) can be accommodated

At sub-zero temperatures, the tensile strength of borosilicate glass tends to increase and equipment can be used with safety at cryogenic temperatures.

Appendix I: Solution Stacking Method of Battery Assembly

This was the first method we attempted for building our batteries. This method involved the sequential stacking of each battery component inside of a half-assembled battery housing.

The process for building the batteries using this process is as follows:

- 1) Aluminum current collector was sealed onto glass tube battery housing
- 2) Cathode slurry was injected into battery housing, building on top of the aluminum current collector
- 3) Cathode was dried in a 60 °C oven for 24 hours, and was compressed into housing after drying using finger strength pressure applied to an aluminum peg
- 4) PGE separator solution was injected into battery housing on top of dried cathode. A very thin layer of PGE was injected, in order to prevent over flow and to minimize separator thickness.
- 5) PGE separator was dried in a 60 °C oven for 12 hours
- 6) Anode slurry was injected into battery housing on top of dried PGE separator and was then allowed to dry in a 60 °C oven for 24 hours. Minimal compression was applied to anode in order to prevent damaging other internal components.
- 7) Battery was moved into argon glove box and liquid electrolyte was injected into battery to saturate the PGE separator and the electrodes.
- 8) The copper current collector was inserted into the battery and finally sealing was completed by applying a layer of Loctite epoxy to junction of copper current collector and glass battery housing.
- 9) After curing of epoxy, battery was removed from glove box and a strip of black electrical tape was wrapped around the battery to act as light shielding.